ERDC/CHL TR-01-15

Coastal and Hydraulics Laboratory

US Army Corps of Engineers®
Engineer Research and Development Center

Hydrodynamic and Sediment Transport Study of Sudbury River, Massachusetts

Numerical Model Investigation

Gregory H. Nail and David D. Abraham

August 2001

20011026 094

ERDC/CHL TR-01-15
August 2001

Hydrodynamic and Sediment Transport Study of Sudbury River, Massachusetts

Numerical Model Investigation

by Gregory H. Nail, David D. Abraham

Coastal and Hydraulics Laboratory
U.S. Army Engineer Research and Development Center
3909 Halls Ferry Road
Vicksburg, MS 39180-6199

Final report

Approved for public release; distribution is unlimited

Prepared for U.S. Army Engineer District, New England
696 Virginia Road
Concord, MA 01742

Contents

Preface

This study was performed by the Hydraulics Laboratory (HL) of the U.S. Army Engineer Waterways Experiment Station (WES), now known as the Coastal and Hydraulics Laboratory (CHL) of the Engineer Research and Development Center (ERDC). The work was done for the U.S. Army Engineer District, New England during May 1994 to December 1996 under the direction of Mr. Thomas W. Richardson, Acting Director, CHL, Mr. Thomas J. Pokrefke, Acting Deputy Director, CHL, Dr. Yen-His Chu, Chief of the River Sedimentation Engineering Branch, and Dr. Robert McAdory, Chief of the Tidal Hydraulics Branch.

The field data collection effort was performed by Mr. Tim Fagerburg, Research Hydraulic Engineer, and Mr. Thad Pratt, Physicist, CHL. Mr. Sam Varnell and Mr. Joseph Parman, Civil Engineering Technicians, CHL, assisted in the field data collection effort.

The numerical modeling effort was completed by Dr. Gregory H. Nail and Mr. David D. Abraham, Research Hydraulic Engineers, CHL. Acknowledgment is made to Mr. Gary Morin, Project Manager, New England District, for cooperation and assistance throughout the the investigation and preparation and review of the report. Special thanks also goes to Mr. Steven Simmer, Hydraulic Engineer, New England District, for his assistance with local hydrologic data.

At the time of publication of this report Dr. James R. Houston was Director of ERDC, and COL John W. Morris III, EN, was Commander and Executive Director.

1 Introduction

The Sudbury River in eastern Massachusetts was the subject of a numerical modeling study and field work which was sponsored and supervised by the U.S. Environmental Protection Agency (EPA). The entire project was interdisciplinary in nature. Therefore it involved scientific and technical personnel from a number of Federal agencies and laboratories in a coordinated effort. The EPA Region I originally contacted the U.S. Army Engineer District (USAED), New England, regarding participation in the study. Consequently, the U.S. Army Engineer Research and Development Center (ERDC), was requested by the New England District to carry out a hydrodynamic and sediment transport study. This report summarizes all work conducted by ERDC as part of the overall project.

The Sudbury River and several of its reservoirs have been exposed to chemical waste effluents from the Nyanza Chemical Waste Dump site in Ashland, MA. The purpose of the overall EPA study was to determine the extent of mercury contamination in existing river sediments and the potential for resuspension and movement of those sediments. Specifically, the purpose of this portion of the EPA study was to determine, with the aid of a hydraulics and sediment transport model, the potential for resuspension and transport of mercury-contaminated sediments within Reservoirs 1 and 2 on the Sudbury River.

The entire EPA investigation area extended from the Nyanza site to the confluence with the Assabet River in Concord, MA. The focus of this report was limited to Reservoirs 1 and 2, immediately downstream of the Nyanza site (Figure 1), on the Sudbury River. These reservoirs were built in 1878 for water supply purposes. They have a surface area of 0.49 and 0.47 km^2 respectively. The combined total drainage area for the two reservoirs is 195 km^2. The upstream reach of Reservoir 2, which is approximately 1.5 km downstream from the Nyanza Site, discharges directly into Reservoir 1. The discharge of Reservoir 1 forms the continuation of the Sudbury River.

2 Field Investigation

Background

The Sudbury Reservoir study was initiated in the spring of 1994. ERDC personnel conducted a reconnaissance trip to Framingham, MA to identify locations of equipment deployment, staging areas, and data collection ranges. At that time, contact was made with individual property owners for permission to access the property and to allow for installation of equipment.

Data Collection

Field data collection efforts were initiated on 24 May 1994 with the setup of the data collection ranges and the boats. The safety procedures for the collection of the bottom samples were affirmed and the locations of the samples were then determined with the aid of a hand-held Global Positioning System. The locations for bottom sampling are shown in Figures 2 and 3. The water level within each reservoir was monitored from recording staff gauges near the existing dams. A small staff gauge was installed near the staging areas to document changes in the water surface elevation during the data collection effort.

Bottom sediment samples (box-core and push-core) were obtained at 15 locations as indicated in Figures 2 and 3. Two types of sampling devices were used to collect the bottom material samples. A Wildlife Supply Company (WILDCO) 6-in. box-core sampler was used to collect undisturbed samples used in the erosion and shear stress testing. The other sampler was a push-core sampler which collects up to a 45.72-cm (18-in.) sample for use in material classification and particle sizing. The push-core sampler was also used to collect grab samples. Grab samples were collected at 15 locations as indicated on Figures 2 and 3. The samples were kept cool and shipped back to ERDC for refrigerated storage until laboratory analysis could be performed. The locations where box-core, push-core, and grab samples were collected are denoted by B, P, and G, respectively (Figures 2 and 3).

Current measurements and water samples were collected on 25-27 May 1994. Velocity profiles at four data collection ranges in each reservoir were obtained over a 12-hr period each day using Acoustic Doppler Current Profiler (ADCP) equipment. Staff gauge readings were monitored during the data collection effort. Several bathymetry data lines were obtained during this period while moving from range to range. The velocity data collected over this period were returned to ERDC for further processing and analysis. Water samples for suspended sediment analysis were collected at two to three stations per range and one to three depths per station. These samples were refrigerated and shipped back to ERDC for laboratory processing to determine the total concentration of suspended sediment in each.

A second field data collection effort was conducted on 13-16 November 1994. Two Endeco water-level recorders were deployed near the gate house on each reservoir. They recorded the water elevation at 10-min intervals. A staff gauge was also attached to each instrument mounting bracket for visual determination of changes in water elevation. Three additional undisturbed bottom samples were collected at previously sampled locations for supplemental laboratory analysis. The laboratory analyses determined the critical shear stress required to initiate erosion and the corresponding erosion rate.

Current measurements and water samples were collected 14-16 November. A complete set of ADCP transects and water samples were collected each day. All samples and data were shipped back to ERDC for analysis and processing. Staff gauge readings were recorded.

Field Results

Data analysis of the velocity profiles obtained from the ADCP revealed that the velocity ranges were 0-30 cm/sec (0-1.0 fps). This was true for both the May and November field data sets. The volume rate of flow occurring in the Sudbury River system at the time these measurements were taken was relatively small; therefore, the low values for velocity measurements were expected. Because the velocity measurements yielded such small magnitudes, meaningful comparisons with computational modeling results were not possible at these low-flow conditions (and were therefore not attempted). Similarly, the plots of velocity magnitudes (from the ADCP transects) are not informative (since they show almost entirely zero or near zero velocity magnitudes). Therefore, the velocity measurements resulting from ADCP transects are not shown. No significant storms or other hydrologic events occurred during either of the data collection periods.

The water samples were processed at ERDC to determine the concentration of suspended sediment in g/L. The values found ranged from approximately 0 to a maximum of 0.033 g/L. The vast majority of samples were found to have a concentration of less than 0.010 g/L.

The distribution of suspended sediment concentration varied little over both Reservoirs 1 and 2. However, the concentrations near Dam 1 were found to be slightly greater than those elsewhere. They ranged from 0.002 to about 0.033 g/L. The average was about 0.005 g/L. Values from samples nearest the bottom usually yielded the highest suspended sediment concentrations.

The values of suspended sediment concentration were found to be slightly lower in the upper reaches of Reservoir 2 than elsewhere. All samples taken from this area were found to yield concentrations of less than 0.004 g/L. The average was about 0.003 g/L.

Finally, bottom material was tested for erosional characteristics using a Particle Entrainment Simulator (Teeter, Parchure, and McAnally 1994). These tests determined that erosion began for most samples at a shear stress of about 0.2 Pa. At a shear stress of 0.5 Pa all samples had experienced some particle erosion. The average rate of erosion at 0.4 Pa was 0.002 $kg/m^2/min$. At 0.6 Pa the rate of erosion increased dramatically for all samples to an average of 0.01 $kg/m^2/min$. Laboratory analysis revealed that the bottom material was mostly clay.

3 Computational Modeling

Background

The computational hydraulics model of the Sudbury River Reservoirs 1 and 2 was developed utilizing field data and other information from various sources. Work on the computational model began soon after the first ERDC field data collection effort was undertaken in the spring of 1994. The Resource Management Associates-2 (RMA-2) model of the TABS-Multi Dimensional (TABS-MD) system of finite-element computational hydraulics and constituent transport models were used.

The RMA-2 model is one of a series of numerical models that form the TABS-MD system (Thomas and McAnally 1990). Elements of the TABS system were developed by ERDC, Resource Management Associates of Lafayette, California, University of California at Davis, and the Brigham Young University Engineering Computer Graphics Laboratory. The RMA-2 model computes water levels and flows using a finite element method to solve the two-dimensional Reynolds form of the Navier-Stokes equations for conservation of mass and momentum. The model requires the user to generate a finite-element mesh which serves as the framework on which the numerical solution is computed. Along the boundary of the domain the user is required to specify volumetric flows either in or out, or water-surface elevation. The model then computes the water-surface elevation and velocities for all interior nodes and nodes along the boundary that are not part of the boundary conditions.

The water-surface levels and velocities from RMA-2 are used by the sediment transport code SED2D. SED2D (Letter et al. 1998)[1] is also part of the TABS-MD system and specifically computes sediment transport, deposition and erosion spatially and temporally over the previously described user-generated finite element mesh. Both SED2D and RMA-2 are depth-averaged models.

[1] J. V. Letter, L. C. Roig, B. P. Donnell, W. A. Thomas, W. H. McAnally, and S. A. Adamec, Jr. (unpublished). "A user's manual for SED2D-WES, a generalized computer program for two-dimensional, vertically averaged sediment transport," draft report, U.S. Army Engineer Waterways Experiment Station, Vicksburg, MS.

Mesh Generation

The first step in developing any finite-element computational hydraulics model is that of mesh generation. The finite-element mesh is a numerical network describing the flow domain. Numerous locations throughout the reservoirs were each assigned coordinate pairs and bottom elevations. Each of these locations is called a node. The entire collection of nodes is joined together into triangular and quadrilateral elements to form a finite-element mesh. It is this mesh that forms the framework upon which the numerical computations are performed. A considerable amount of effort was directed towards obtaining the best possible mesh at the earliest date practical. Bathymetry data were obtained from field surveys conducted by ERDC and the United States Geological Survey (USGS), Marlborough, MA.

The finite element meshes have 1,086 nodes and 325 elements for Reservoir 1 and 2,198 nodes and 665 elements for Reservoir 2. The finite element mesh for Reservoir 1 is shown in Figure 4. Figure 5 shows the mesh developed to describe Reservoir 2.

The integrity of the meshes was tested by using the RMA-2 code to simulate progressively more complicated and longer duration hydrographs, beginning with steady-state flows. Eventually, complete hydrographs describing the flows during real events were used as input boundary conditions. During this process of tuning and adjusting parameters, the meshes were edited slightly several times.

Hydrodynamic Modeling

Boundary conditions (inflows in cfs) were specified at the extreme upper reaches of the meshes representing Reservoirs 1 and 2, as well as at the submerged gates (by the dams), when necessary. For Reservoir 1 (Figure 4) one inflow is specified at the upstream location which corresponds to the outflow from Reservoir 3 (Figure 1). The other upstream reach on the south end of Reservoir 1 is an inflow boundary condition that corresponds to the outflow from Reservoir 2. The remaining boundary conditions specified are that of the pool stage (in ft) near Dam 1, as well as flow (in cfs) through the submerged gates by Dam 1.

Similar information was supplied to the computational hydraulics model of Reservoir 2 (Figure 5). An inflow (cfs) was specified at the extreme end of the upper reach. The pool stage (ft) near Dam 2 was specified. Flow (cfs) through the submerged gate near Dam 2 could have been specified also, but was not necessary for the events reported here (the gate by Dam 2 was closed). The inflows and stages were supplied to the model for every time-step (3 hr).

The RMA-2 model computes velocity and depth at each node throughout the mesh for each time-step. A time-step and initial conditions for head (throughout the mesh) must be specified. A Manning's n roughness coefficient is assigned based on local depth and ranged from 0.02 up to about 0.08 for the shallowest areas of the mesh. A turbulence model was used that required eddy viscosities to be specified. These were computed based on a historically accepted and successful scaling relationship using a locally calculated Peclet number (P) as shown in Equation 1. The local velocity is u, density is ρ, the local elemental dimension is dx, and E is the resulting eddy viscosity. This scaling relationship causes the eddy viscosity, throughout most of the hydrograph for the various cases, to range typically from 0 - 287 Pa-sec (0 - 6 lb-sec/ft^2). Higher values are usually computed at nodes with higher velocity magnitudes. Typical values of eddy viscosity were in the range from 95.8 to 192 Pa-sec (2.0 to 4.0 lb-sec/ft^2). However, in regions of locally high (greater than 152 cm/sec (5 fps)) velocity magnitudes the eddy viscosities were occasionally as high as 1440 to 1920 Pa-sec (30 to 40 lb-sec/ft^2) or higher. The eddy viscosity scaling relationship is described in detail in the recently updated documentation on the RMA-2 model (Donnell et al. 1998). The eddy viscosities are updated as the computational algorithm proceeds:

$$P = \frac{\rho\ u\ dx}{E} \tag{1}$$

Output from the model includes velocities and depths, at each node throughout the mesh, for each time-step. At any particular cross section the volumetric discharge can be determined. The discharges through each dam were computed from RMA-2 in this fashion and compared with field-obtained data supplied by the New England District. When an acceptable level of agreement with field data was observed for two representative cases, the model was considered to have been verified.

Four hydrographs were supplied by the New England District for testing the hydraulic model. These hydrographs were developed using the Hydrologic Engineering Center program, HEC-1. This program was previously verified to field results. HEC-1 is a well accepted one-dimensional computational model that uses rainfall intensity and basin characteristics to compute a basin outflow hydrograph. The RMA-2 model was run using the same inflow and outflow boundary condition values as the HEC-1 simulation. The computed discharges from the RMA-2 model should match those computed by HEC-1. Since the HEC-1 model has been previously verified to field results, when the RMA-2 results agree with it, the RMA-2 model can also be considered to be verified in a one-dimensional flow-routing sense. Some RMA2 and HEC-1 model results are shown in Figures 6 through 9.

Figures 6 and 7 show comparisons of RMA-2 and HEC-1 results for the Standard Project Flood (SPF). The RMA-2 code was run for 40 separate 3-hr time-steps for a total simulation time of 120 hr. The entire 40 time-step sequence constitutes one computer run for RMA-2. At each of these time-steps the flow over Dam 1 was computed. In both figures note that the curve representing RMA-2 is very close to that of HEC-1 at all points in the hydrograph. No flow was present through the gate in either Dam 1 or Dam 2 for the SPF.

A similar result is depicted in Figures 8 and 9 for a recent flood event that occurred in August 1991. The gate in Dam 1 was operated during this time and its flow has been supplied to RMA-2. The effect of opening the gate can be seen in the slight dip in the discharge curve as shown for RMA-2 on Figure 8 near hour 93. This same feature is not seen in the HEC-1 primarily because it is not able to completely account for gate flow. In spite of this note the close agreement between RMA-2 and HEC-1 is shown in Figure 8. Figure 9 depicts excellent agreement between RMA-2 and HEC-1 for Reservoir 2. No gate flow occurred through Dam 2 during the August 1991 event.

Figures 8 and 9 show maximum discharges over the spillways, as computed by the New England District, for the August 1991 event. The maximum for Reservoir 1 is about 21.2 cu m/s (750 cfs) (with an additional gate discharge of 6.37 cu m/s (225 cfs) for a total outflow of 27.6 cu m/s (975 cfs)). The maximum for Reservoir 2 is 12.2 cu m/s (430 cfs). Figures 6 and 7 show that the maximum discharges for the SPF reached 292 and 147 cu m/s (10,300 and 5,200 cfs), in Reservoirs 1 and 2, respectively. Note that the discharges reported for these two events are an order of magnitude different. Use of these two events as test cases provided a wider range of flows over which to evaluate model performance.

Due to the hypothetical nature of the SPF event, velocity measurements were not available for comparison with RMA-2 predictions. Although the August 1991 event was real, no velocity measurements were taken. Consequently, evaluation of RMA-2 predictions of velocity distribution were not possible for either case.

Sediment Transport Modeling

The sediment transport model SED2D requires sediment boundary conditions as well as previously generated hydrodynamic information from RMA-2 as input. The boundary conditions include initial suspended sediment concentrations at each node in the computational mesh in addition to those along inflow boundaries corresponding to the RMA-2 hydrodynamic solution. Also, information about the river or streambed is required by SED2D. The SED2D model is an improved version of the STUDH model. For details refer to Thomas and McAnally (1990).

SED2D is capable of simulating either sand or clay. In this case clay was selected, and the parameters describing Reservoirs 1 and 2 bed material, were given to the model as input. The model accepts information about the bottom in a schematized series of layers, each with its own specific erosion and deposition characteristics. All of this information is usually not precisely known. However, engineering judgment and experience are relied on to supply reasonable values where they are not known a priori.

SED2D runs for a series of time-steps in a manner similar to RMA-2. It computes bed elevation change, bottom shear stress, and suspended sediment concentration at each node in the finite element mesh for each time-step. The cumulative bottom elevation change is tallied for each node as computation proceeds through the hydrograph. The entire field of cumulative bed elevation change serves as a useful parameter from which model performance can be evaluated.

For the SED2D results, the initial and inflow boundary suspended sediment concentrations for both reservoirs were set to 0.001 g/l. The bottom was described by a simple representation of two layers. The critical shear stress (see Equation 2) required to initiate particle erosion in the surface layer was set equal to 0.4 Pa. The particle erosion rate constant was set to 0.0020 $kg/m^2/min$. These parameters, obtained from laboratory experiments on sediment from the site, were used to describe the uppermost layer of the bed everywhere in the model.

The top layer of sediment over most of the bed in both reservoirs was assumed to be 0.5 m deep. In places where the shores of the reservoir form a natural (or manmade) constriction, the depth of this top layer was reduced to 1 mm. In locations forming transitions between these two areas the thickness of the top layer of sediment was specified as 3 cm.

It was decided, on the basis of previous experience and observation, to treat flow constrictions in the manner previously described. Any flow constriction formed by natural or manmade features causes locally higher velocities. Therefore, higher bottom shear stresses occur at that location. It is therefore common to observe that, in the vicinity of constrictions in open channel flow, the bottom is relatively hard. The faster moving water tends to keep the constriction scoured. The thinner top layer supplied to the model will tend to erode away quickly when exposed to high velocities. However, the harder material beneath will erode slowly.

The scheme of prescribing a relatively thin top layer along the bottom in flow constrictions allows the sediment transport model to realistically simulate the limited scouring that occurs in these areas. As the more easily eroded material is removed, the more compacted and less easily eroded material is exposed. In this way the natural process of armouring is simulated.

A second layer underneath the top layer was specified at all places in the model for an additional depth of 10 m beneath the top layer. Its parameters were set to simulate material that is compacted and significantly more difficult to erode (critical shear stress of 0.6 Pa and particle erosion rate constant of 0.00012 $kg/m^2/min$). A third layer was specified under the entire bed that was even more difficult to erode (critical shear stress of 50.0 Pa and particle erosion rate constant of 0.000060 $kg/m^2/min$). The third layer was never reached by erosion during any sediment transport model run. However, its presence is necessary for proper operation of the SED2D program.

The representation of stable bed erosion for clay utilized by SED2D is based on that of Krone (1962), and is shown in Equation 2. The critical shear stress for particle erosion is τ_c, while the depth is D and the laboratory-determined particle erosion rate constant is P (not to be confused with Peclet number described earlier). Consequently, Equation 2 gives a resulting rate of erosion S for any given local shear stress τ.

$$S = \frac{P}{D}\left(\frac{\tau}{\tau_c} - 1\right) \quad (2)$$

No field-obtained values of erosion and deposition throughout the reservoirs were available. As a consequence, evaluation of the accuracy of SED2D predictions of these quantities was not possible.

Results and Discussion

In qualitative terms, the results of the study to date indicate that sediments in Reservoirs 1 and 2 will be moved for various flood frequencies as follows:

a. The 3-year flood (represented by the 1991 historical flood event), and the 14-year flood (represented by the 1987 historical flood event) cause negligible movement of sediments.

b. The 100-year flood (represented by the 1955 historical flood event) causes some movement of sediments.

c. The 1,000-year flood (represented by the SPF) causes substantial movement of sediments.

Most of the movement of sediments occurred near constrictions, or narrow and shallow portions of the reservoirs. No significant movement of sediments was detected in the deeper sections of the reservoirs.

Scour will normally occur when the velocities in a water body produce bottom shear stresses in excess of the critical shear stresses. For the material samples taken from the bottom of these reservoirs, and subsequently tested, that critical shear stress was determined to be 0.4 Pa. Based on this information and the calculated velocities, the sediment transport model is able to compute accumulations and/or removal of sediments at all nodal locations in the computational network.

Specifically, referring to item a, for the 14-year event, the amounts of scour and/or deposition that occurred in Reservoirs 1 and 2, can be viewed in Figures 10 and 11, respectively. Positive values indicate deposition whereas negative values indicate erosion. Note in Figure 10 that any measurable amount of sediment movement occurred only in areas of constrictions and at the outflow to the submerged gate next to the dam. The scour predicted at the gate was 54 cm (1.8 ft) and was by far the maximum for the entire reservoir. The sediment transport and hydraulic models are limited in their ability to properly resolve the details of flow through a three-dimensional feature, such as a submerged gate. Also, the grid resolution was not made fine enough to resolve a detail as small as the outflow pipe. For these reasons, the scour shown here is believed to be significantly greater than would actually occur. Therefore, scour predicted in the vicinity of the gate is not generally used in evaluating the potential for contaminated sediment transport. As shown in Figure 10 (7.6 cm (0.25 ft) contour interval) scour for the remainder of the bottom was predicted to be less than 7.6 cm (0.25 ft). The zero contours in the constrictions (Highway 9 Bridge and Salem End Road Bridge) indicate that scouring has occurred at these locations. However, the absence of a 7.6-cm (0.25-ft) contour indicates that the scour was less than 7.6 cm (0.25 ft). The maximum deposition predicted in Reservoir 1 for the 14-year event is 0.62 cm (0.020 ft), just downstream of Dam 2.

As shown in Figure 11, the maximum scour predicted in Reservoir 2 for the 14-year event is in the vicinity of the Conrail R.R. Bridge. Scour of 18 cm (0.60 ft) is shown at this location. The maximum deposition predicted is 0.43 cm (0.014 ft), just upstream of Dam 2. The absence of 7.6 cm (0.25 ft) contours on the rest of Figure 11 indicates that scour elsewhere (Fountain Street Bridge) in Reservoir 2 is less than 7.6 cm (0.25 ft). The place names (Highway 9 Bridge, etc.) and locations of Dams 1 and 2 labeled on Figures 10 and 11 also apply to Figures 12 through 19.

The scour patterns of Figures 12 and 13 clearly shows predicted erosion for the 3-year event to be less at all locations in both reservoirs than those for the 14-year event.

Referring to item b, the 100-year event, and Figure 14, the maximum depth of scour predicted in Reservoir 1 was 19 cm (0.63 ft) near the Highway 9 Bridge. As can be seen in Figure 14, fairly large areas downstream of the Highway 9 and Salem End Road Bridges have experienced scour. However, the absence of the 7.6 cm (0.25 ft) contour indicates that all of this scour was less than 7.6 cm (0.25 ft). The maximum scour that did occur in these areas was 3.1 cm (0.10 ft), just downstream of the Salem End Road Bridge. In Reservoir 2, (Figure 15) the maximum scour of 23 cm (0.75 ft) occurred in the upstream end of the reservoir near the constriction formed by the Conrail R.R. Bridge. The zero contours, but absence of 7.6 cm (0.25 ft) contours, in the reach beginning just downstream of the Fountain Street Bridge and extending to just downstream of the Conrail R.R. Bridge indicates that scour in these areas was less than 7.6 cm (0.25 ft) at all locations. The maximum deposition predicted for Reservoir 2 for the 100-year event is 0.95 cm (0.031 ft) just downstream of the Fountain Street Bridge.

Note that the actual length of simulation time was significantly less (114 hr) for the 100-year event than for the 14-year (228-hr) and 3-year (192-hr) events. The gates were operated for each event and the flows through the gates were similar in magnitude. However, the longer period of record (longer simulation time) allowed for the computation of somewhat greater depths of erosion in the vicinity of the gates for the 3-year and 14-year events, as compared to the 100-year event. This can be seen by noting the scour contours near the gate next to Dam 1 on Figures 10 and 12 (14-year and 3-year events) with those of Figure 14 (100-year event).

Referring to item c, the SPF, and Figure 16, the maximum scour predicted for Reservoir 1 occurs in two localized areas. On the north bank downstream of the Highway 9 Bridge, local scour reaches a maximum of 52 cm (1.7 ft). Another area of scour reaches a maximum of 52 cm (1.7 ft) downstream of the Salem End Road Bridge. The predicted maximum deposition was 8.3 cm (0.27 ft) near the confluence of the two main reaches of Reservoir 1. In Reservoir 2 (Figure 17) a maximum scour of 52 cm (1.7 ft) is predicted just downstream of the Conrail R.R. Bridge. Local areas of scour ranging upwards to 31 cm (1.0 ft) are shown in Figure 17 in the reach between the Conrail R.R. and Fountain Street Bridges. The maximum deposition predicted for the SPF for Reservoir 2 was 9.8 cm (0.32 ft) in a local area just downstream of the Fountain Street Bridge. Another local maximum deposition of 8.6 cm (0.28 ft) is predicted a little further downstream of the Fountain Street Bridge. This area is visible in Figure 17 by the 7.6-cm (0.25-ft) contour. The hydrodynamic results showed this location to be the center of a recirculation zone. The gates were not in operation for this hypothetical case.

Having presented the information showing the movement of sediments for the various flood frequencies, the most important questions to be answered can now be addressed. Do contaminated sediments move, and if so, where and in what quantities?

Figure 18 shows the locations where bottom samples were taken from Reservoir 1 for determination of mercury concentrations in the sediments. All samples taken are not shown. The samples with the highest concentrations, which are in parts per million (ppm), are shown to illustrate a worst case scenario. All but four samples were taken by NUS Corporation as part of Nyanza Operable Unit III, Phase 1 and 2. A total of four samples were taken by USGS (Frazier et al. 2000), three in Reservoir 2 and one in Reservoir 1. One of the samples taken by USGS in Reservoir 1 showed significantly higher amounts of mercury than those taken by NUS Corp. It is not known if these differences are due to sampling techniques and/or laboratory analysis methods. What is evident is that at the two locations of maximum scour in Reservoir 1 for SPF, sediments are scoured to a depth of approximately 37 cm (1.7 ft), as shown in Figure 16. At these locations, according to Figure 18, sediments containing mercury at values of 2.0 and 6.1 ppm are about 15 and 16 cm deep in the profile. Therefore they would be entrained and transported during an event with discharges equaling those of the SPF. It should be noted that the levels of mercury concentration in the sediments vary in the vertical profile. An assumption is being made in this study that the highest concentration of mercury in the sediments in general, falls between 12 to 15 cm down in the sediment profile. Accordingly, Figures 16 and 18 show that the only other location in Reservoir 1 where contaminated sediments might be entrained, for the SPF, is approximately just downstream of Dam 2. The depth of scour predicted in this area is about 15 cm (0.50 ft). The highest concentration of these sediments is noted as 4.3 ppm and are located 15 cm deep in the profile.

For Reservoir 1 none of the other conditions (3-year, 14-year, or 100-year) cause enough scour to reach contaminated sediments anywhere other than locally at the Highway 9 Bridge. The only case (other than SPF) that shows any potential of scouring contaminated sediments is the 100-year event with local scour of 15 cm (0.50 ft) at the Highway 9 Bridge just sufficient to reach mercury concentrations of 2.0 ppm in sediment 15 cm deep.

Figure 19 shows the distribution of bottom samples taken for determining mercury concentration in Reservoir 2 sediments. As before, all samples taken are not shown. The samples with the highest concentrations are shown. Figure 19 clearly shows that the reach of river between Fountain Street Bridge and the Conrail R.R. Bridge contains bottom sediment mercury concentrations of up to 75 ppm at depths of 12 to 26 cm (0.4 to 0.85 ft). Figure 17 shows the predicted scour depth in this reach locally reaches 31 cm (1.0 ft) for the SPF conditions. Therefore, it is clear that for the SPF conditions any contaminated sediments residing within 31 cm (1.0 ft) of the bed surface in this area will be entrained and transported. Scour patterns for the 100-year and 14-year events show local scouring just reaching or exceeding 12 cm (0.4 ft) locally near the Conrail R.R. Bridge. Therefore, some limited resuspension of contaminated sediments, at this location only, could be expected to occur as a result of either of these events.

Dam Break Modeling

At the request of the EPA, a scheme was devised to model the effects of a dam break scenario. The hydrodynamic and sediment transport computational models described previously were modified to simulate the hydrodynamic and sediment transport responses to the sudden removal of the dam(s). The RMA-2 and SED2D programs are not designed to handle the three-dimensional effects or wave propagation, especially in the vicinity of the dam, characteristic of a dam break scenario. Other one, two, and three-dimensional hydrodynamic models with this capability exist. However, as of the date of this report a similar cohesive sediment transport model (that can accommodate dam break conditions) is not known to be readily available.

A dam break scenario was approximated by modifiying the existing models of Reservoir 1 and 2 to simulate a quick drawdown. This was accomplished primarily by removing elements from the finite-element mesh. The finite-element meshes used for the dam break simulations are shown in Figures 20 and 21. A comparison with Figures 4 and 5 will readily show the differences in the meshes. Notice that the removal of elements was exclusively along the banks and in shallow areas or adjoining small tributaries. During the extremely low-water levels characteristic of a dam break scenario, much of the near-bank and shallow areas become dry. This is typically handled by the RMA-2 hydrodynamic program quite easily, although it does cause numerical instabilities. However, the numerical instabilities caused by this procedure (while running the SED2D sediment transport program) were found to be significant. In some cases the computations diverged.

It was reasoned that, since the shallow areas quickly become dry during a dam break scenario, they would make only minor contributions to the total sediment resuspended. Removal of computational elements along these areas was justified in this way. Therefore, all the elements shown in the meshes of Figures 4 and 5, that remain wet throughout the entire simulation, were retained. The elements that become dry were removed, and new meshes were developed (Figures 20 and 21) specifically for the dam break scenario. In this way the numerical instabilities were greatly reduced, while only slightly affecting the final result.

The dam break models require the same boundary and initial conditions as do the previously described models. The inflow hydrographs were developed by the New England District and are shown in Figures 22 and 23 for Reservoirs 1 and 2, respectively. Figures 24 and 25 show the corresponding pool stages of Reservoirs 1 and 2. Figures 22 through 25 approximate a potential catastrophic total failure of Dam 2, during a 100-year flood event, immediately followed by the total failure of Dam 1. The inflows of Figures 22 and 23, together with the stages of Figures 24 and 25 together constitute hydrodynamic boundary conditions for the dam break scenario. This scenario was selected in an attempt to approximate or exceed the very worst case (failure of Dam 2, shortly thereafter followed by failure of Dam 1 under record high flow rates) conditions that could possibly be expected. The conditions illustrated by Figures 22 through 25 were used as boundary conditions for the hydrodynamic model to run the dam break simulation. Since these conditions represent only a hypothetical event, it was not possible to verify or validate the model quantitatively. However, care was taken to see that all results appeared reasonable and consistent. This qualitative way of monitoring model performance was done primarily because a more rigorous verification of the model (featuring comparisons with field data) would not be possible.

Note the sudden peak discharge (to over 227 cu m/s (8,000 cfs)) from Reservoir 2 on the plot of Figure 22. This feature clearly depicts the time of occurrence of the failure of Dam 2 (at about hr 6). Note the corresponding drop in Reservoir 2 pool stage shown in Figure 25. A jump in the pool stage of Reservoir 1, as shown on Figure 24, can be seen to correspond with the sudden peak discharge from Dam 2, shown in Figure 22. Note that the hydrographs of Figures 22 through 25 each extend to 30 hr. The hydrographs clearly show that, by hour 30, the highest of the discharges (with the most erosive effects) have already occurred. Therefore, the dam break simulation was run only up to and including hour 30. A 0.25 hr time-step was used.

The only modification in the sediment transport model was that of specifications of the bed sediments. An extra (fourth) 10-m-deep layer was added beneath the existing bed structure described earlier. The rest of the specifications for the bed sediments and inflowing concentrations were unchanged.

The results of the dam break scenario previously described are shown in Figures 26 and 27. These figures show the predicted scour pattern over the bottom of the reservoirs, at the end of the 30-hr dam break simulation. Note that, although the contour interval is 7.6 cm (0.25 ft), the zero contour is approximated by the 0.0031 cm (0.00010 ft) contour. It was found that this selection of contours caused a somewhat more legible contour plot to be produced by the plotting software. The high velocities and shallow depths produced some (less than 0.0031 cm (0.00010 ft)) scour over all portions of the reservoirs, including the deepest sections.

Note in Figure 27, for Reservoir 2, that there were three areas in which the maximum scour exceeded 46 cm (1.5 ft). These three locations are just downstream of the Conrail R.R. Bridge, the bend above the Fountain Street Bridge, and near Dam 2. The maximum scour in Reservoir 2 was approximately 53 cm (1.8 ft), in the bend previously mentioned. According to Figure 19, all maximum mercury concentrations along the bottom of Reservoir 2 were found 26 cm (0.85 ft) deep or less. Also, Figure 19 indicates that most of these readings showed peaks at depths of 15 cm (0.49 ft) deep into the sediments of Reservoir 2. Figure 27 shows scour depths reached 15 cm (0.49 ft) in only four local areas. The largest of these is in the bend upstream of the Conrail R.R. Bridge. Therefore, the model predicts that mercury-contaminated sediments would be resuspended from these four areas as a result of water currents caused by the hypothetical dam break scenario. Although the bend area upstream of the Conrail R.R. Bridge is localized, the resuspended sediments there are of relatively high mercury concentration (49 ppm) according to Figure 19.

Note that, with the exception of the vicinity of Dam 2, the pattern and depth of scour predicted for Reservoir 2 for the dam break scenario (Figure 27) is similar to that for the SPF (Figure 17). In general, the areas further upstream experience the most scour. This is to be expected, as the velocities increase from shallow depths and high discharges as the pool stage is drawn down. The only exception to this, of course, is in the immediate vicinity of Dam 2.

The predicted scour pattern, resulting from the dam break scenario, is shown in Figure 26 for Reservoir 1. Three local areas of maximum scour are clearly visible near Dam 2, Highway 9 Bridge, and Dam 1. The maximum scour was 50 cm (1.6 ft) just downstream of Dam 2. Note that this irregularly shaped scour hole is in the immediate downstream vicinity of Dam 2. Obviously, this feature has formed as a direct result of exposure to sustained high velocities due to the failure of Dam 2 at Hour 6 (see Figure 22). Elsewhere in Reservoir 1 the scour depth is less than 15 cm (0.5 ft). Figure 18 shows that all maximum mercury concentrations were detected at depths in the sediment 12 cm (0.39 ft) or greater. The predicted depth of scour in all but two of the three isolated areas (Highway 9 Bridge and Dam 2) fails to reach 12 cm (0.39 ft). At these two locations of local maximum scour (exceeding 12 cm (0.39 ft)) nearby sediment samples indicate relatively low level mercury concentrations of 2.0 and 4.3 ppm, respectively. The model predicts resuspension of mercury-contaminated sediments in these two areas resulting from the dam break scenario.

4 Conclusions

Three important facts should be kept in mind at this point. First, we were not able to verify in an absolute sense the sediment model because of a lack of verification data. Second, the locations and concentration of mercury-contaminated sediments are spot samples. It is therefore not known to what extent the contamination covers the entire reservoir bed. Third, the event that caused the most significant amount of contaminated sediment entrainment was the SPF. This flood is a hypothetical creation of some unlikely extreme event which, for this watershed, has a probability of occurring once in every thousand years. There is a 0.1 percent chance of an event of this magnitude occurring in any given year. This event was chosen to illustrate the very worst case scenario.

The TABS-MD system has been used to develop a hydrodynamic and sediment transport model of the Sudbury Reservoirs 1 and 2. The results of the hydrodynamic simulations of RMA-2 show close agreement with HEC-1 and measured data. These hydraulic simulations closely followed both the trends and actual values of discharge computed for Reservoirs 1 and 2 for both SPF and August 1991 events. On the basis of these results it is concluded that the hydrodynamic models are verified. Therefore, output (velocities and depths) from the hydrodynamics can be used as input to the sediment transport models.

The sediment transport models gave reasonable results consistent with experience, engineering judgment, and field observation. The absence of field data for flow versus scour and deposition makes direct comparison with computer predictions from the sediment transport model impossible. A quantitative evaluation of the SED2D sediment transport model cannot be made. However, it is possible to evaluate the SED2D model results in a qualitative sense. It is concluded that the sediment transport model is capable of simulating the movement of sediment through Reservoirs 1 and 2, and identifying areas of actual and potential erosion and deposition resulting from hypothetical storm events.

Similarly, the dam break simulation was done without the ability to quantitatively verify the accuracy of the sediment transport model. Nevertheless, reasonable and consistent predictions of scour and deposition were obtained. It is concluded that the models can provide qualitative results that can be used with engineering judgment to make estimates of the threat of sediment bed erosion in Reservoirs 1 and 2. RMA-2 and SED2D do not trace the individual contaminant particle paths to determine their fate. However, the models do calculate spatially and depth-averaged deposition at each computational node. Therefore, the two-dimensional (horizontal) spatial distribution of erosion and deposition can be estimated.

General conclusions and qualifying statements can now be made regarding the potential for movement of sediments due to the occurrence of hypothetical storm events. The largest amount of entrainment of contaminated sediments will be in Reservoir 2, in its upstream end as previously discussed. Very little entrainment and transport will occur in Reservoir 1. Deposition is predicted in several locations in Reservoir 1 and 2. It is known that some sediments will settle in the reservoir, but some will also be carried over the spillway (and through the dam gates if open).

A more realistic event to consider is the 100-year flood. As indicated by its name, it is a flood which, on the average, is expected to occur once in every 100 years. There is a 1 percent chance this flood event will actually occur in any given year. By comparing the contaminated sediment locations (Figures 18 and 19) with the scour map (Figures 14 and 15), it can be seen that there are no extended areas where scour depth is deep enough to reach contaminated sediments. The maximum depth of scour predicted is locally at the constriction marking the uppermost extreme reach of each reservoir. The predicted maximum scour at these two locations is sufficient to reach contaminated sediments residing there. However, these are at two isolated locations and are not where the highest concentrations are found. The sediment layers with the highest concentrations of mercury may not be entrained. Relatively insignificant scour is predicted over all of the lower reaches and deeper portions of both reservoirs. Once again, the probability of such an event occurring is small. The only recorded event of this magnitude occurred in 1955, as a result of Hurricane Diane.

As expected, the dam break simulation predicted resuspension of sediments would occur in both reservoirs. A comparison of the total area of predicted scour for the SPF and the dam break scenario can be seen by comparing Figures 16 and 17 (SPF) with Figures 26 and 27 (dam break scenario). As shown in these figures, qualitatively speaking, the total area over which resuspension occurs is not significantly greater than that for the SPF. However, it must be cautioned that a dam break scenario, by its very nature, introduces many variables which cannot be known a priori. For example, the amount of sediment resuspended from the erosion of exposed lake bottom is unknown, and could be significant in a sustained, intense storm event. The exposure of large areas of lake bottom could occur hypothetically after a dam break. This situation could lead to significant erosion during the next flood event. However, the modeling and analysis of such an unlikely occurrence is beyond the scope of this study.

References

Donnell, B. P., Letter, J. V., McAnally, W. H., Roig, L. C. (1998). "User's guide for RMA2 version 4.3," (http://chl.wes.army.mil/software/tabs/docs.htp), U.S. Army Engineer Waterways Experiment Station, Vicksburg, MS.

Frazier, B. E, Wiener, J. G., Rada, R. G., and Engstrom, D. R. (2000). "Stratigraphy and historic accumulation of mercury in recent depositional sediments in the Sudbury River," Canadian Journal of Fisheries and Aquatic Sciences 57: (in preparation).

Izbicki, J. A., and Parker, G. W. (1991). "Water depth and thickness of sediment in Reservoirs 1 and 2, Framingham and Ashland, Massachusetts," U.S. Geological Survey, Open-File Report 91-508.

Krone, R. B. (1962). "Flume studies of the transport of sediment in estuarial shoaling processes, final report," Hydraulic Engineering Laboratory and Sanitary Engineering Research Laboratory, University of California, Berkeley.

Teeter, A. M., Parchure, T. M., and McAnally, W. H. (1994). "Size dependent erosion of two silty-clay sediment mixtures," *Cohesive Sediments*, Fourth Nearshore and Estuarine Cohesive Sediment Transport Conference, 11-15 July 1994, Wallingford, England, UK, 253-262.

Thomas, W. A., and McAnally, W. H. (1985). "User's manual for the generalized computer program system: open-channel flow and sedimentation, TABS-2," Instruction Report HL-85-1, U.S. Army Engineer Waterways Experiment Station, Vicksburg, MS.

Thomas, W. A., and McAnally, W. H. (1990). "Open channel flow and sedimentation, TABS-MD," IR-HL-85-1, revised, U.S. Army Engineer Waterways Experiment Station, Vicksburg, MS.

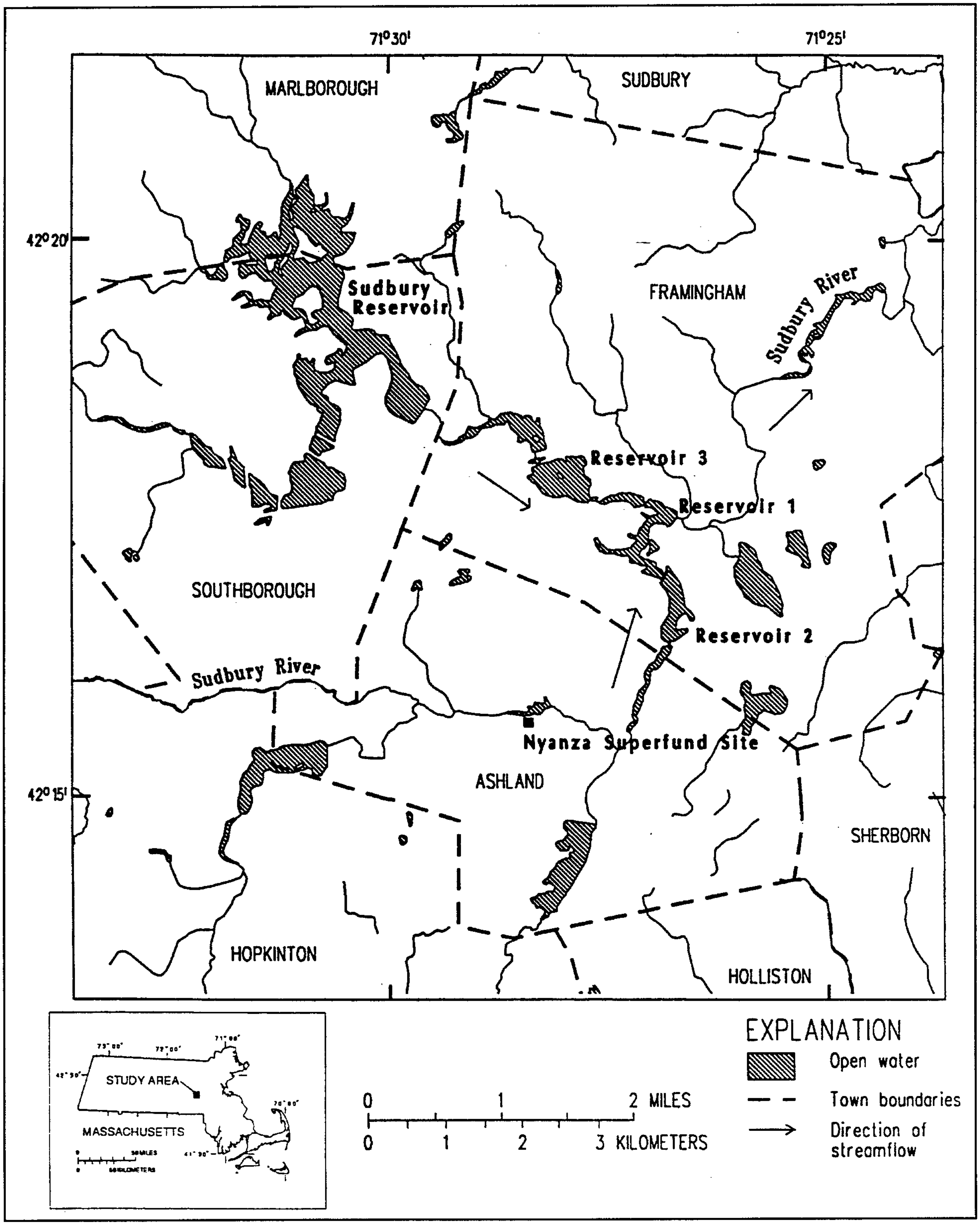

Figure 1. Location of study area (Courtesy of Izbicki and Parker (1991))

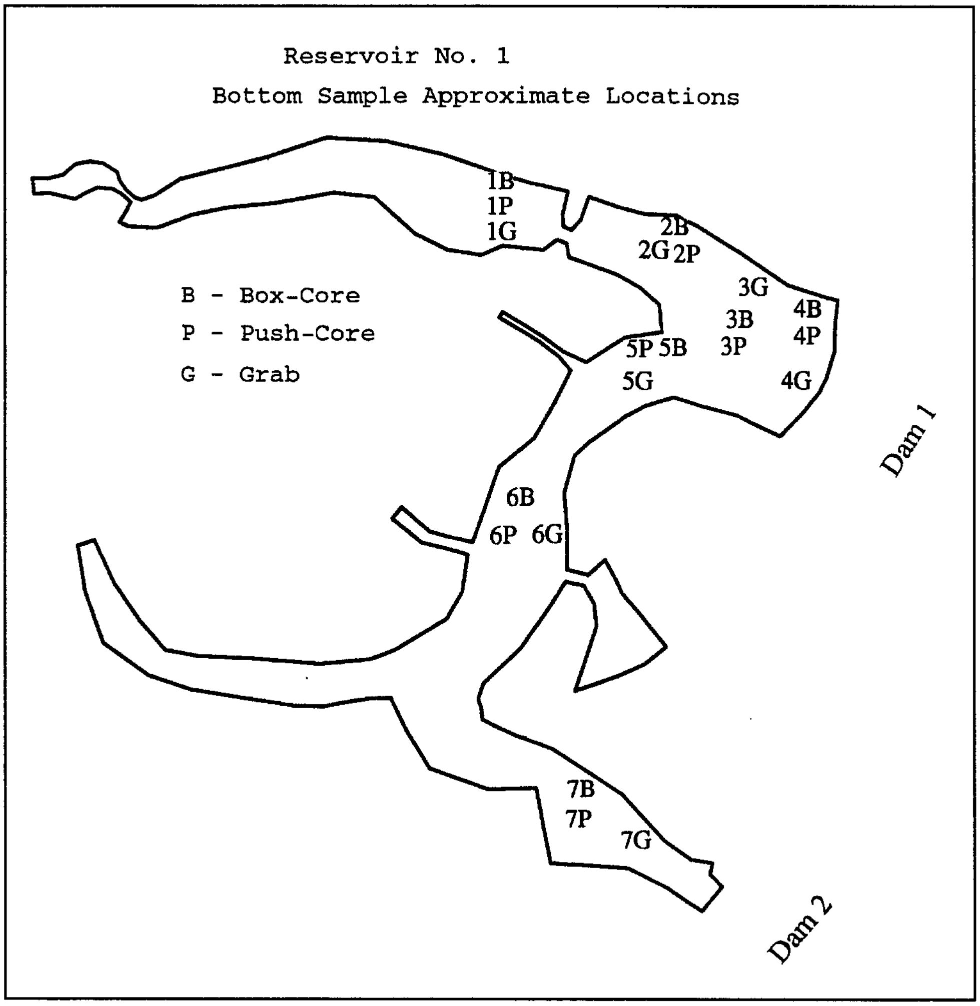

Figure 2. Bottom sampling locations in Reservoir 1

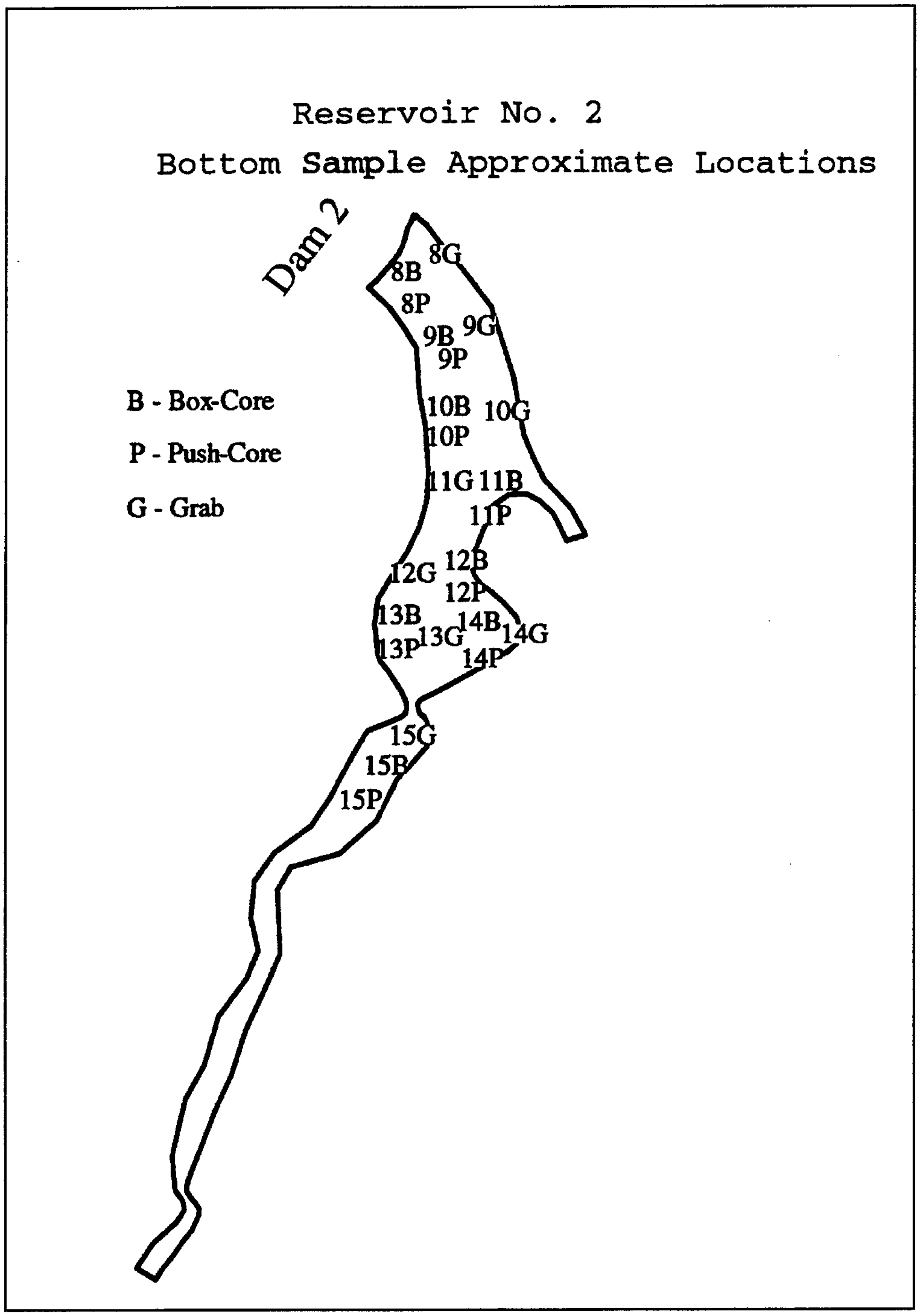

Figure 3. Bottom sampling locations in Reservoir 2

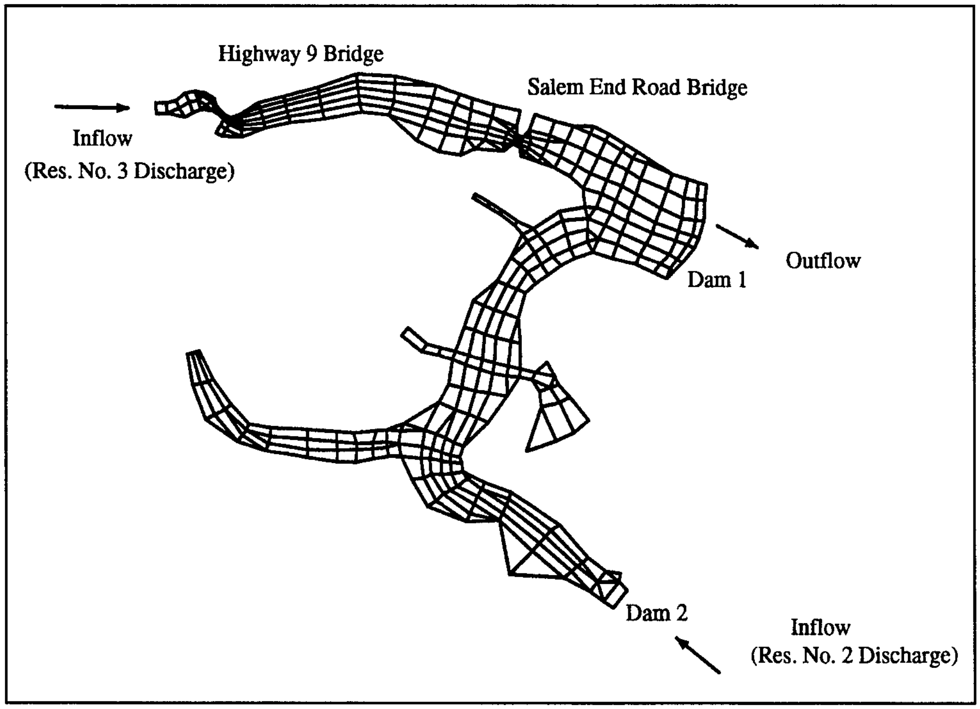

Figure 4. Reservoir 1 finite element mesh

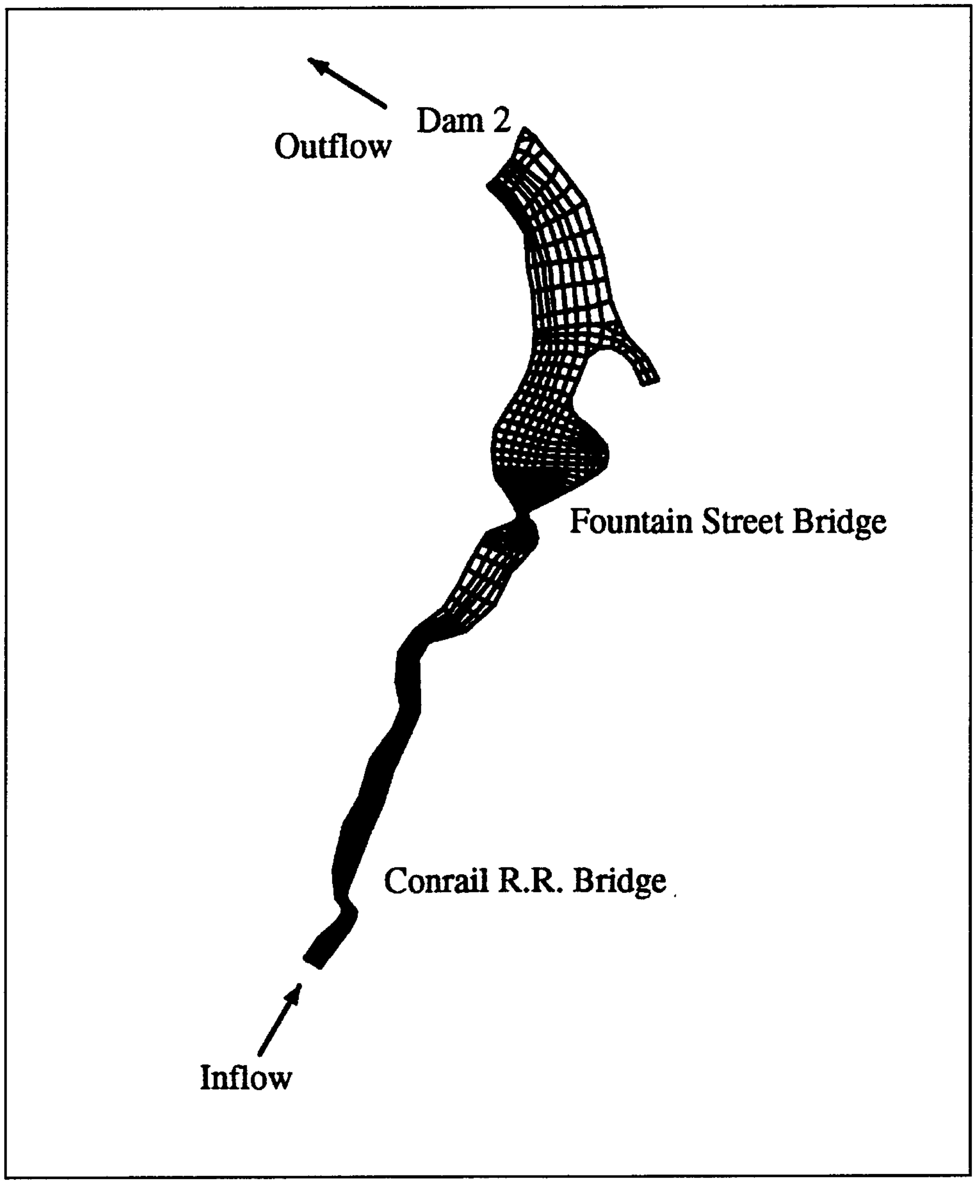

Figure 5.   Reservoir 2 finite element mesh

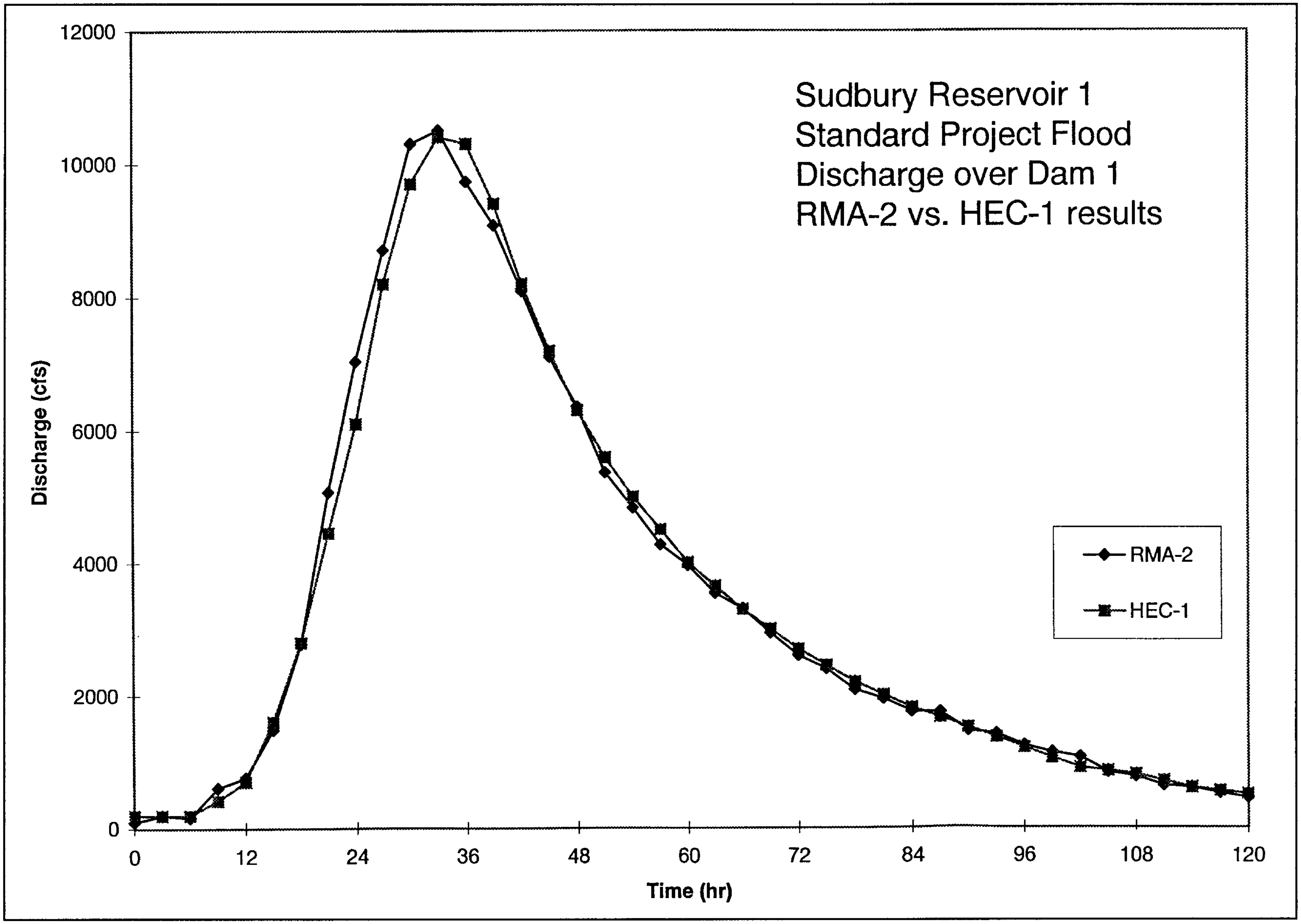

Figure 6. Discharge (Dam 1 Spillway) versus time for Reservoir 1, standard project flood (1,000-year) (Discharge is in cubic feet per second. To convert to cubic meters per second, multiply by 0.0283)

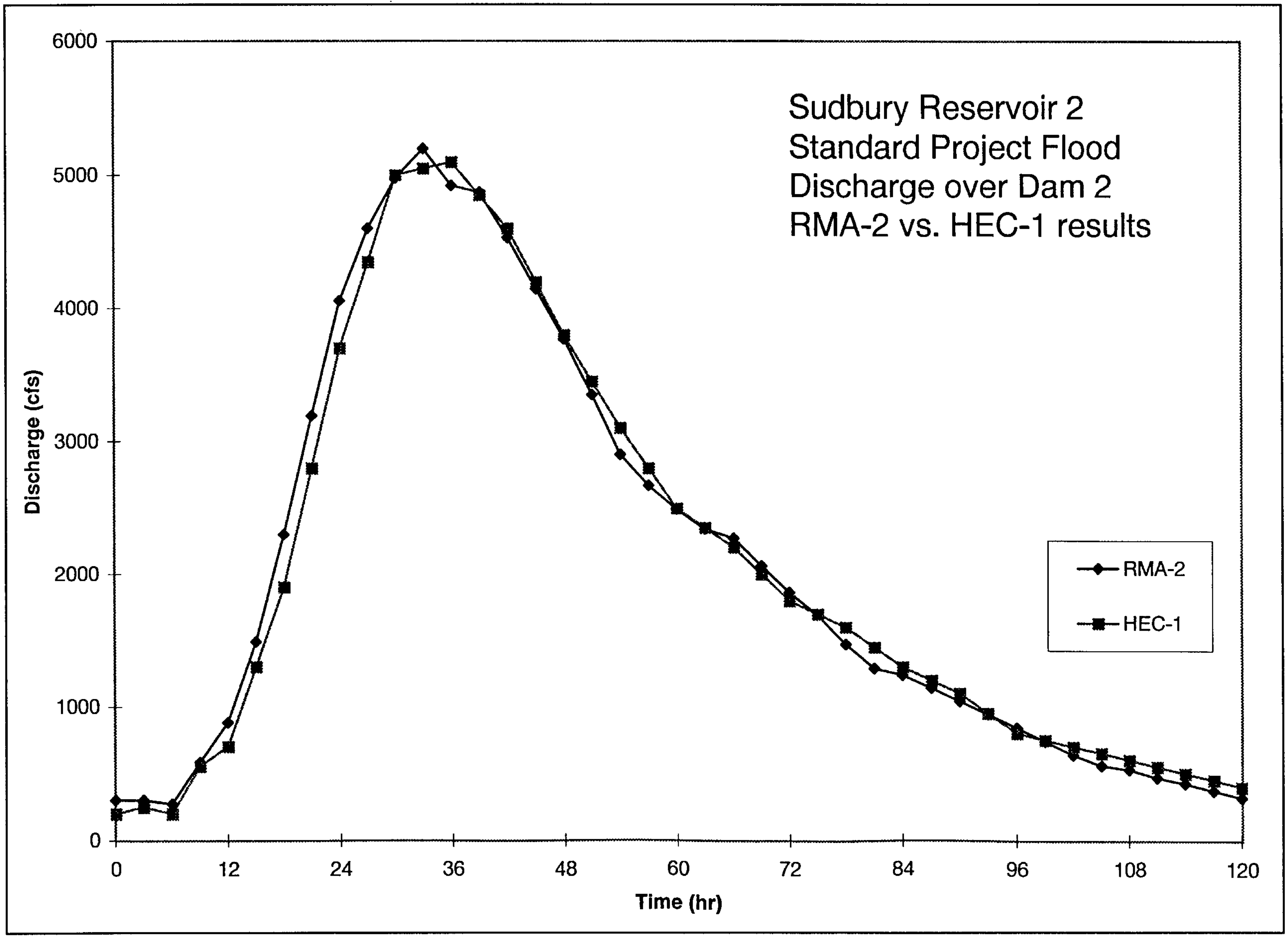

Figure 7. Discharge (Dam 2 Spillway) versus time for Reservoir 2, standard project flood (1,000-year) (Discharge is in cubic feet per second. To convert to cubic meters per second, multiply by 0.0283)

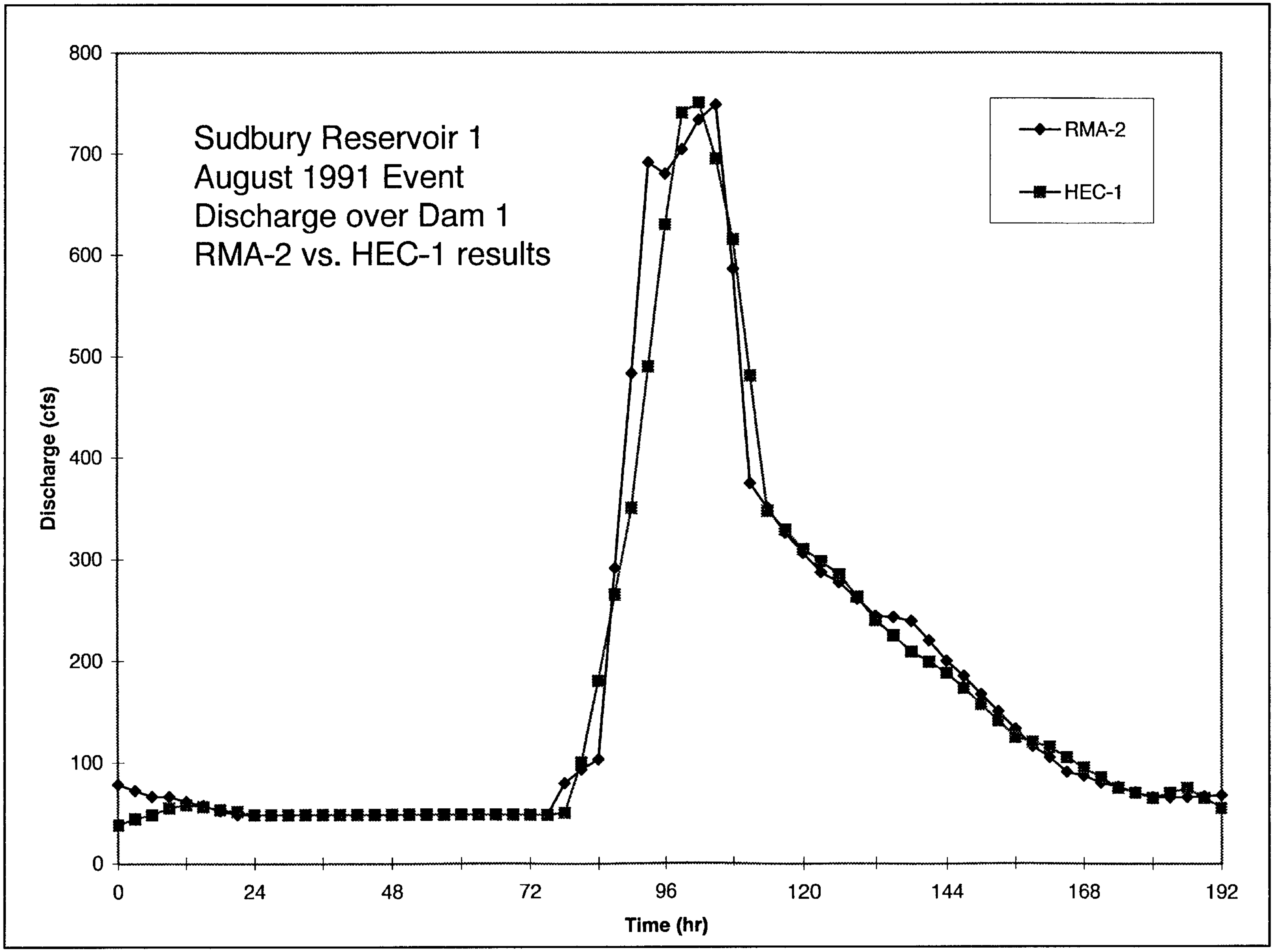

Figure 8. Discharge (Dam 1 Spillway) versus time for Reservoir 1, August 1991 event (3-year) (Discharge is in cubic feet per second. To convert to cubic meters per second, multiply by 0.0283)

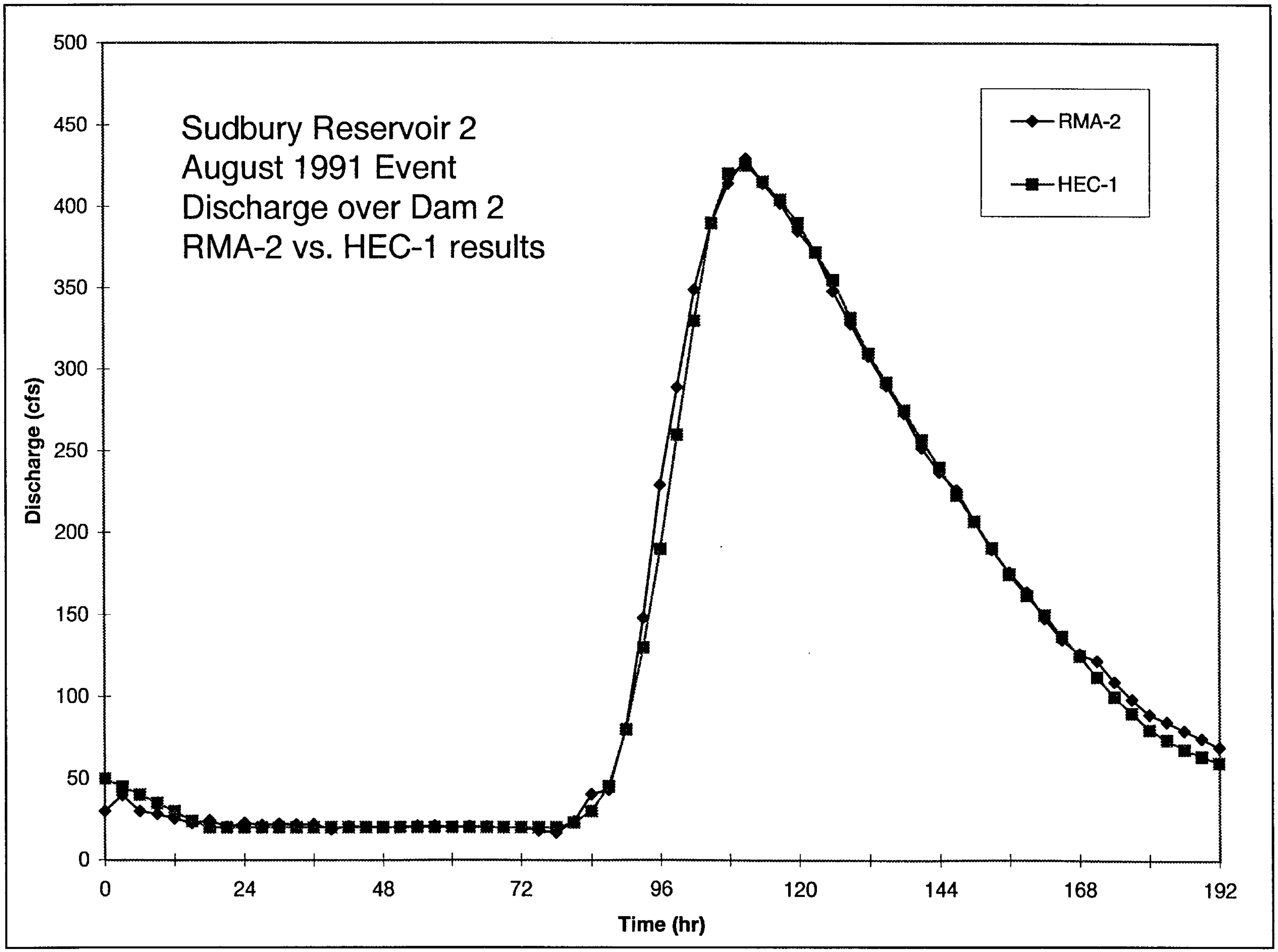

Figure 9. Discharge (Dam 2 Spillway) versus time for Reservoir 2, August 1991 event (3-year) (Discharge is in cubic feet per second. To convert to cubic meters per second, multiply by 0.0283)

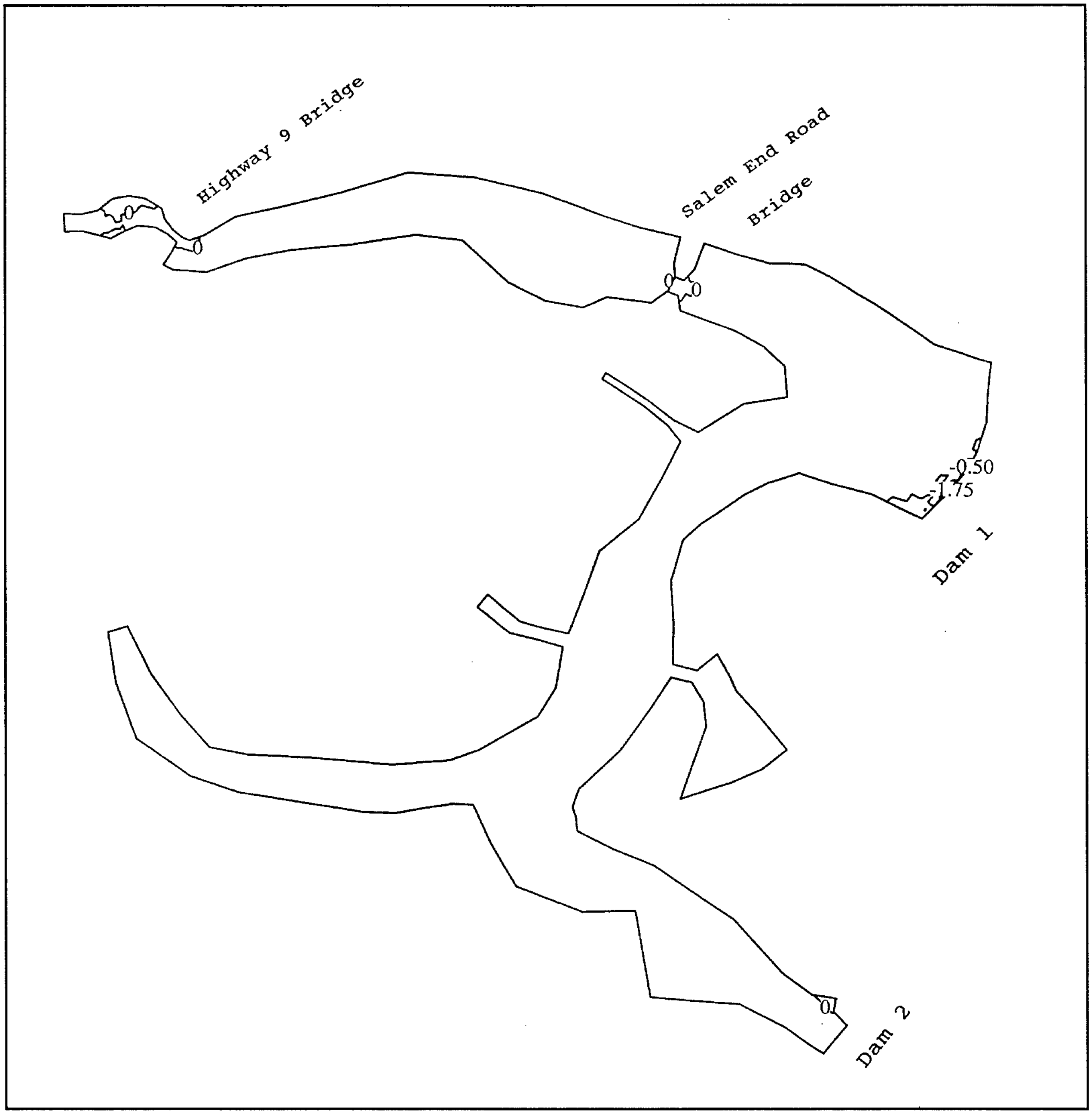

Figure 10. Contours of cumulative bed elevation change (ft), contour interval 0.25 ft, April 1987 (14-year)event (hour 228) Reservoir 1 (To convert feet to meters, multiply feet by 0.3048)

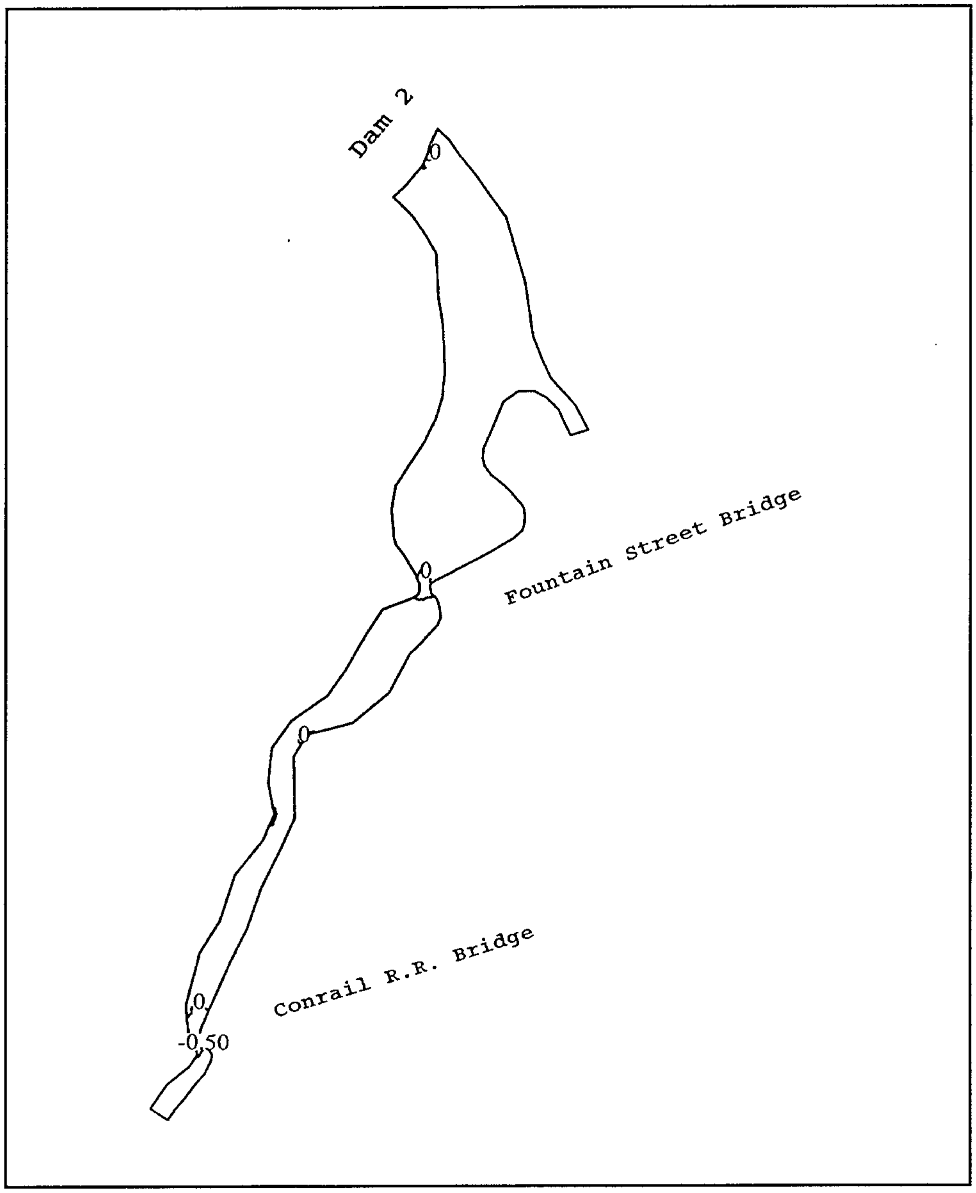

Figure 11. Contours of cumulative bed elevation change (ft), contour interval 0.25 ft, April 1987 (14-year) event (hour 228) Reservoir 2 (To convert feet to meters, multiply feet by 0.3048)

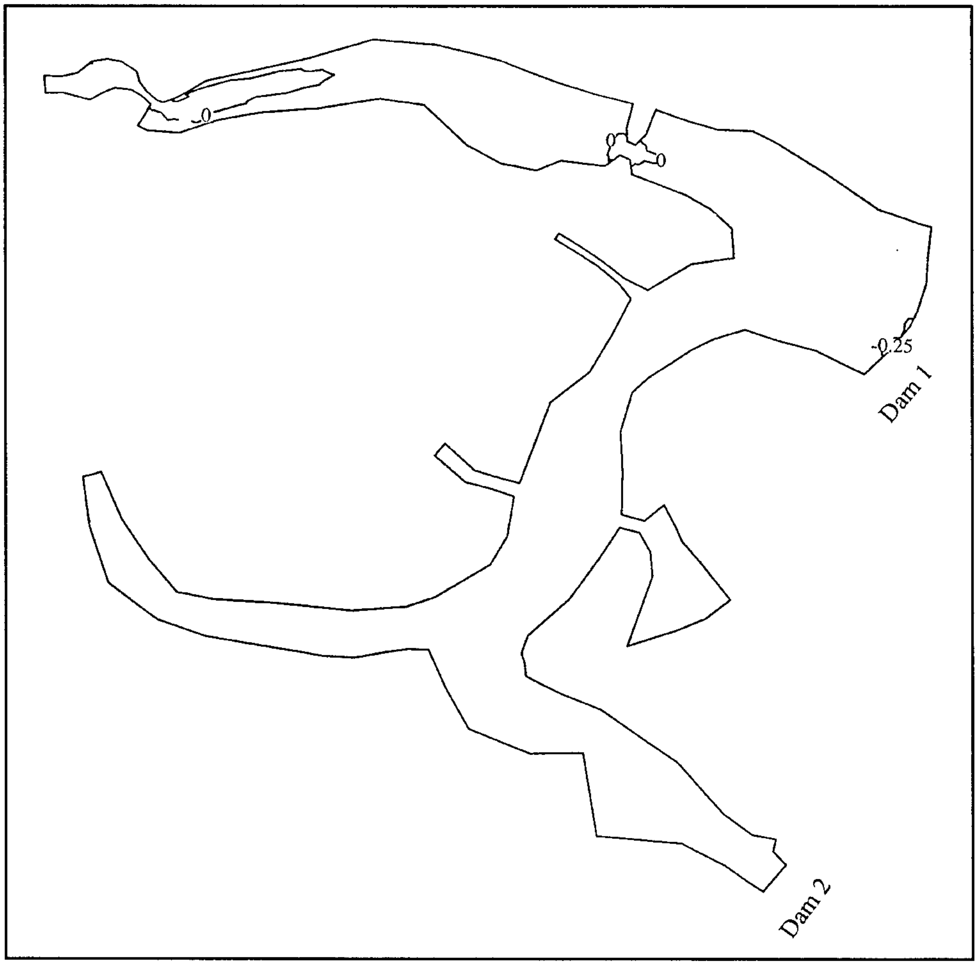

Figure 12. Contours of cumulative bed elevation change (ft), contour interval 0.25 ft, April 1991(3-year) event (hour 192) Reservoir 1 (To convert feet to meters, multiply feet by 0.3048)

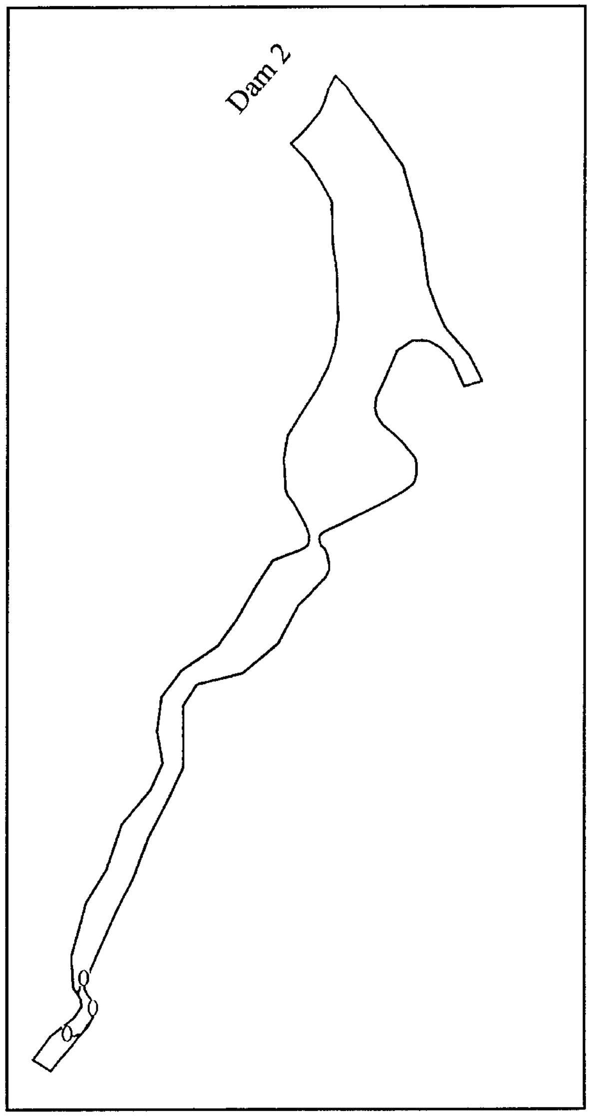

Figure 13. Contours of cumulative bed elevation change (ft), contour interval 0.25 ft, April 1991 event (3-year) (hour 192) Reservoir 2 (To convert feet to meters, multiply feet by 0.3048)

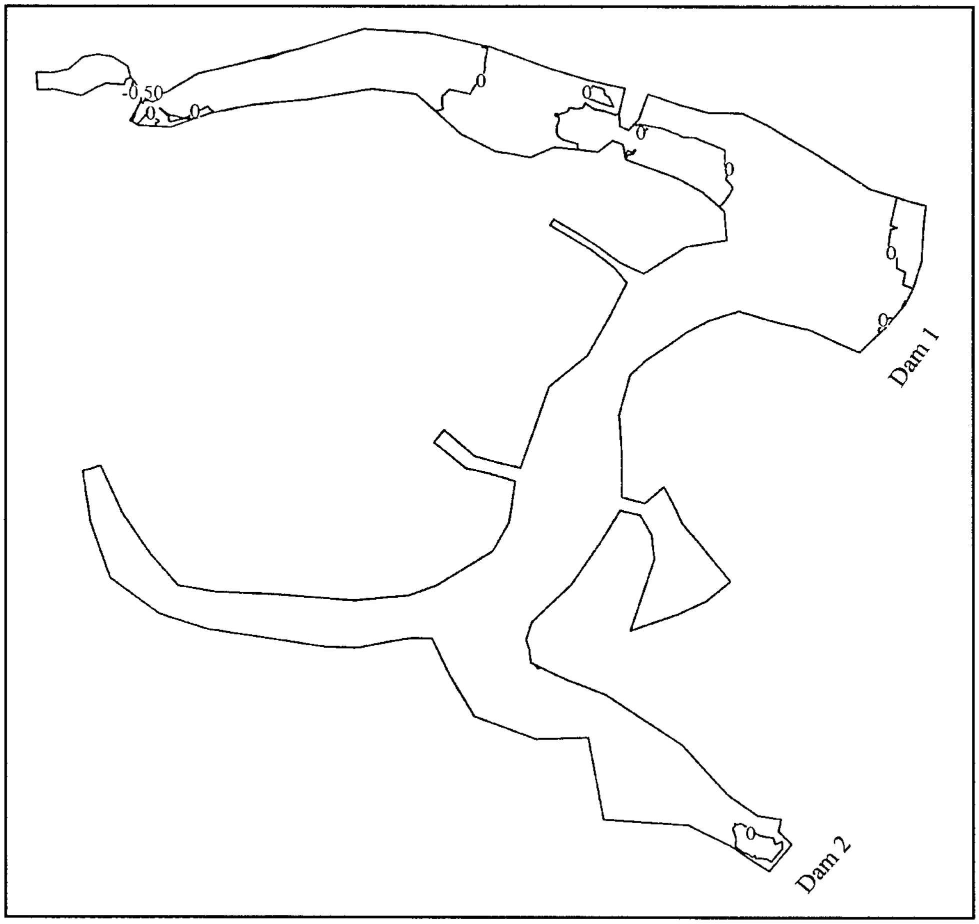

Figure 14. Contours of cumulative bed elevation change (ft), contour interval 0.25 ft, August 1955 event (100-year) (hour 114) Reservoir 1 (To convert feet to meters, multiply feet by 0.3048)

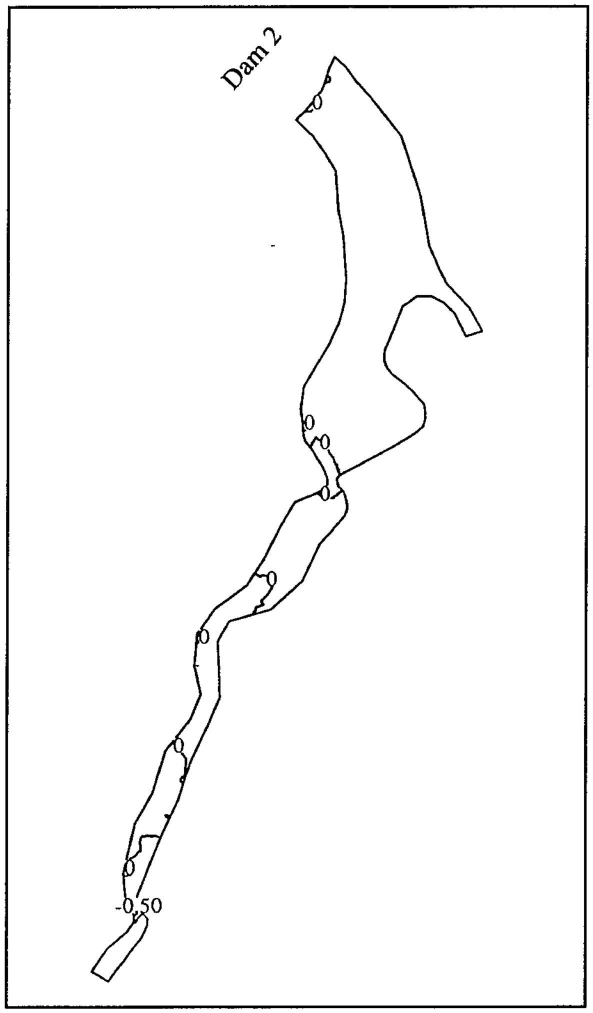

Figure 15. Contours of cumulative bed elevation change (ft), contour interval 0.25 ft, August 1955 (100-year) event (hour 114) Reservoir 2 (To convert feet to meters, multiply feet by 0.3048)

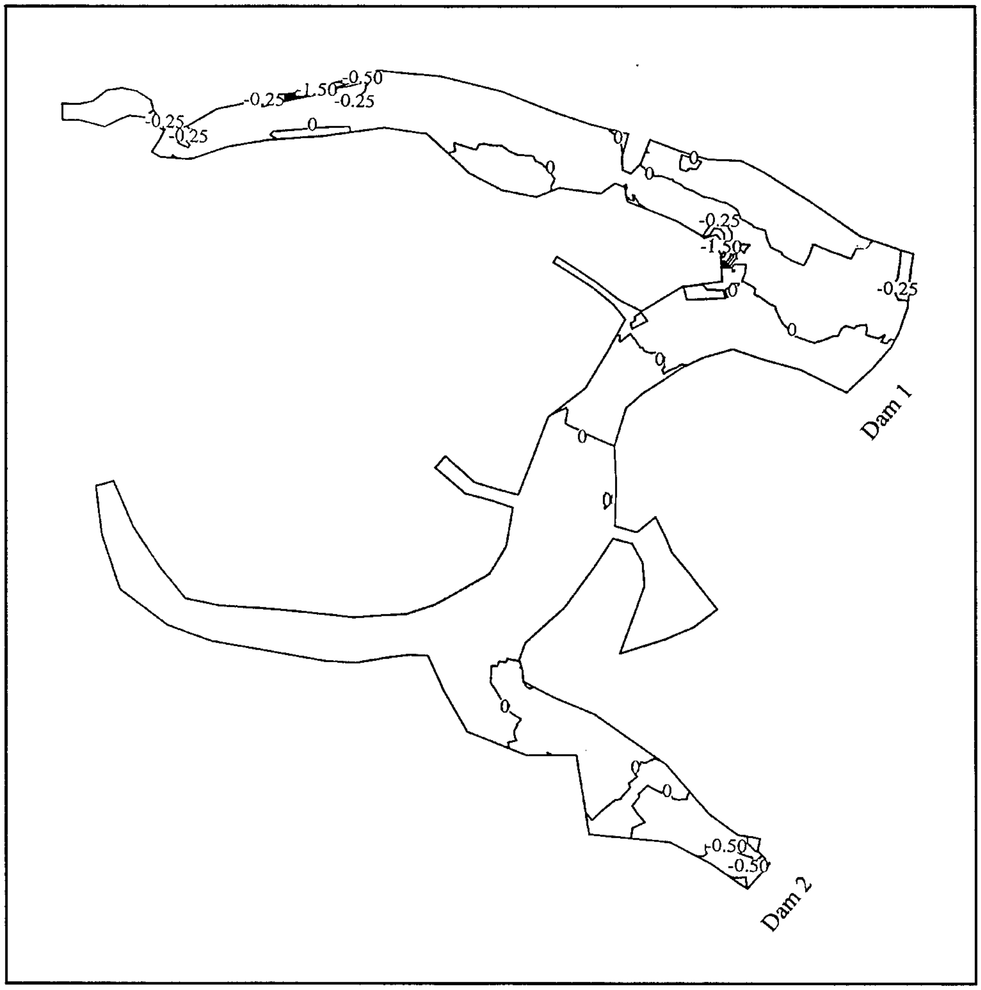

Figure 16. Contours of cumulative bed elevation change (ft), contour interval 0.25 ft, standard project flood (1,000-year) (hour 120) Reservoir 1 (To convert feet to meters, multiply feet by 0.3048)

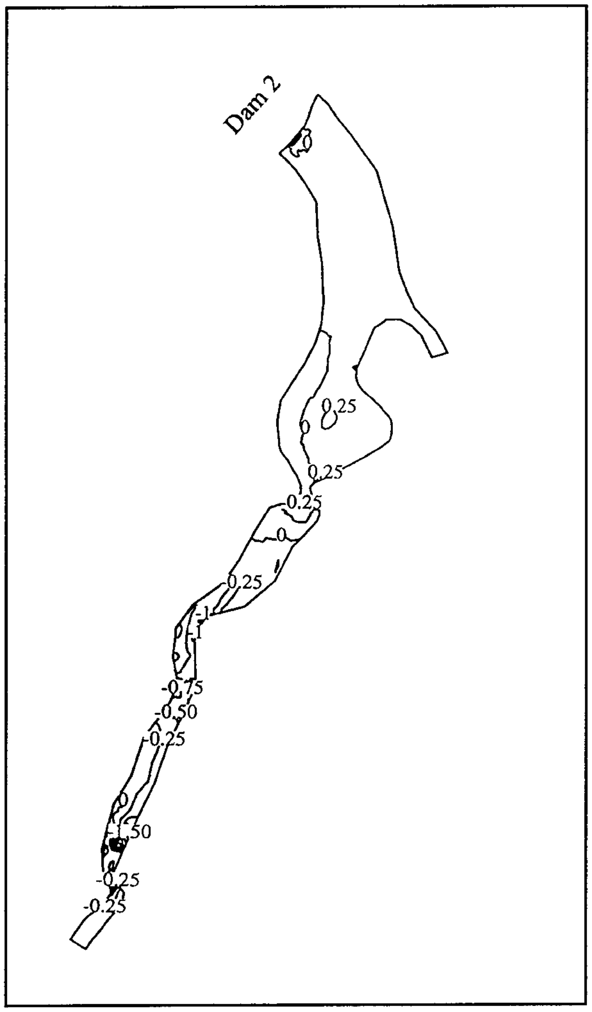

Figure 17. Contours of cumulative bed elevation change (ft), contour interval 0.25 ft, standard project flood (1,000-year) (hour 120) Reservoir 2 (To convert feet to meters, multiply feet by 0.3048)

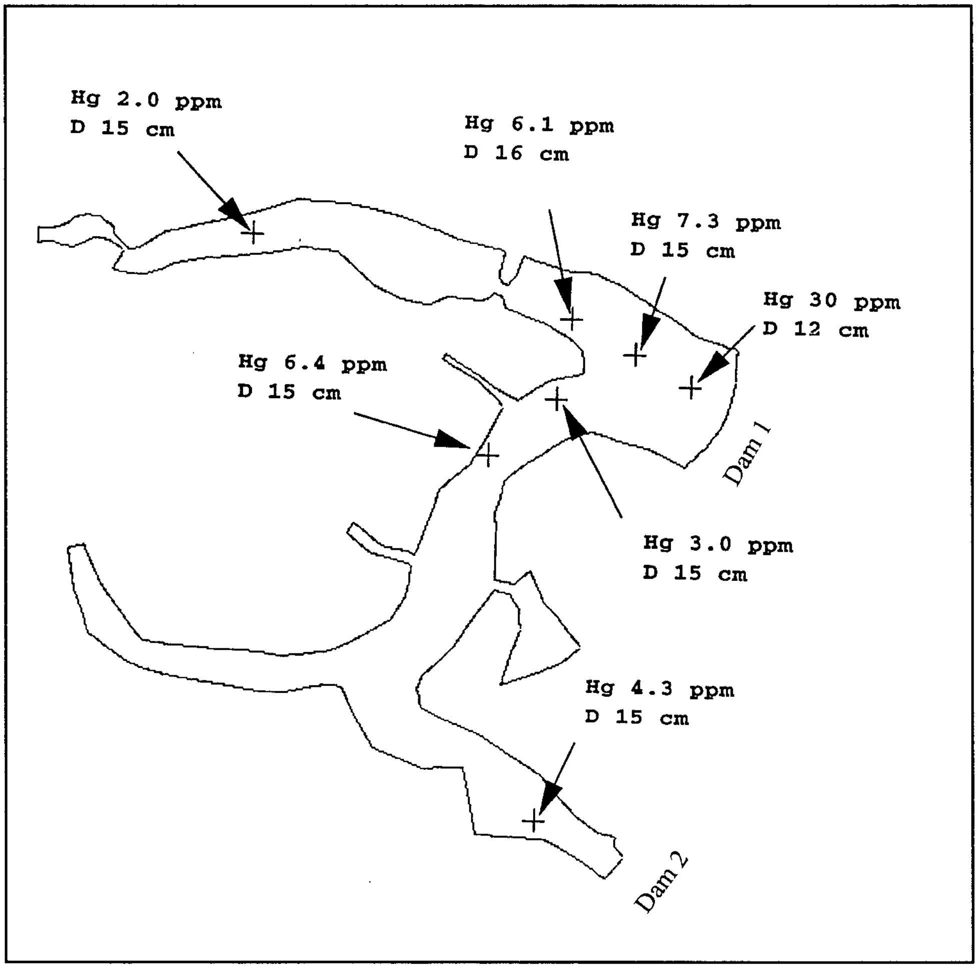

Figure 18. Reservoir 1 bottom sample locations for Hg concentration, maximum Concentrations (Hg) in ppm, depth for each maximum concentration (D) in cm

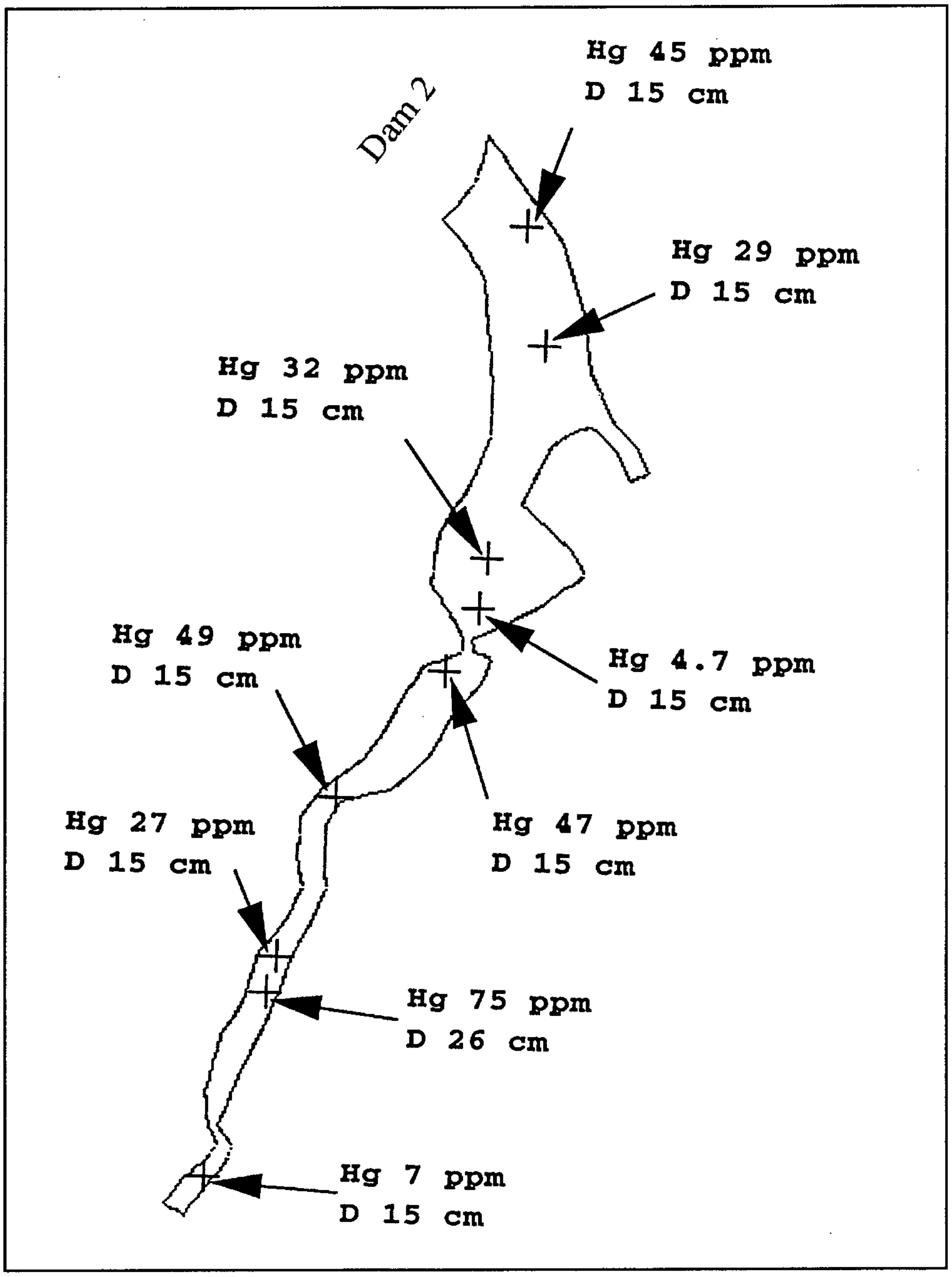

Figure 19. Reservoir 2 bottom sample locations for Hg concentration, maximum Concentrations (Hg) in ppm, depth for each maximum concentration (D) in cm

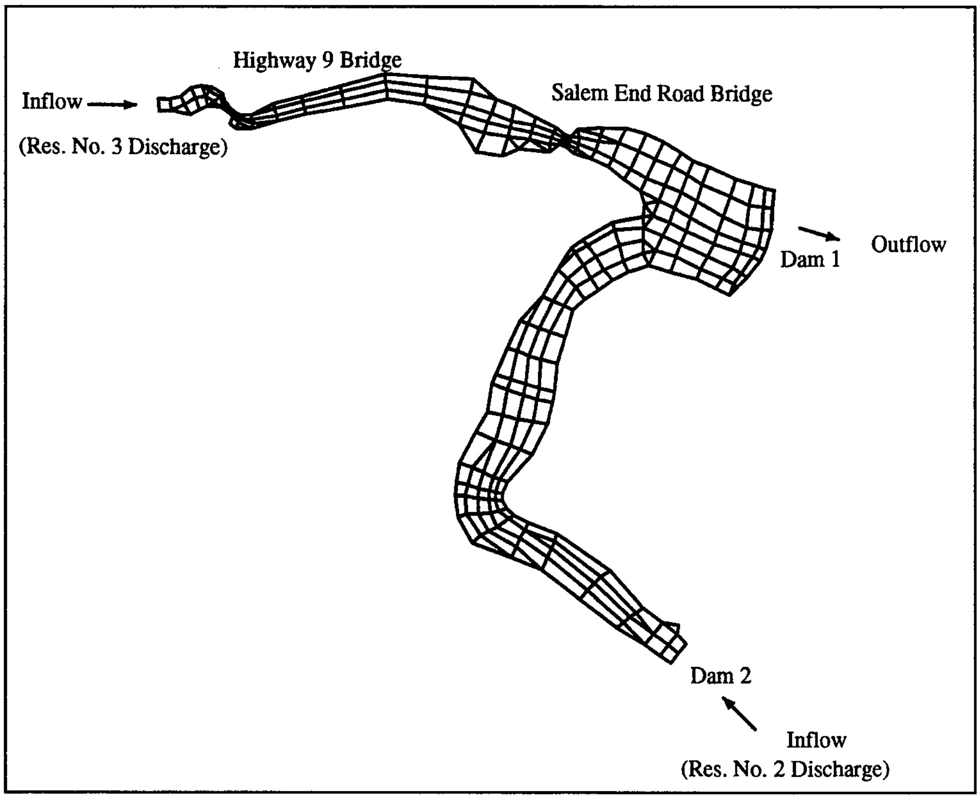

Figure 20. Reservoir 1 finite element mesh, dam break simulation

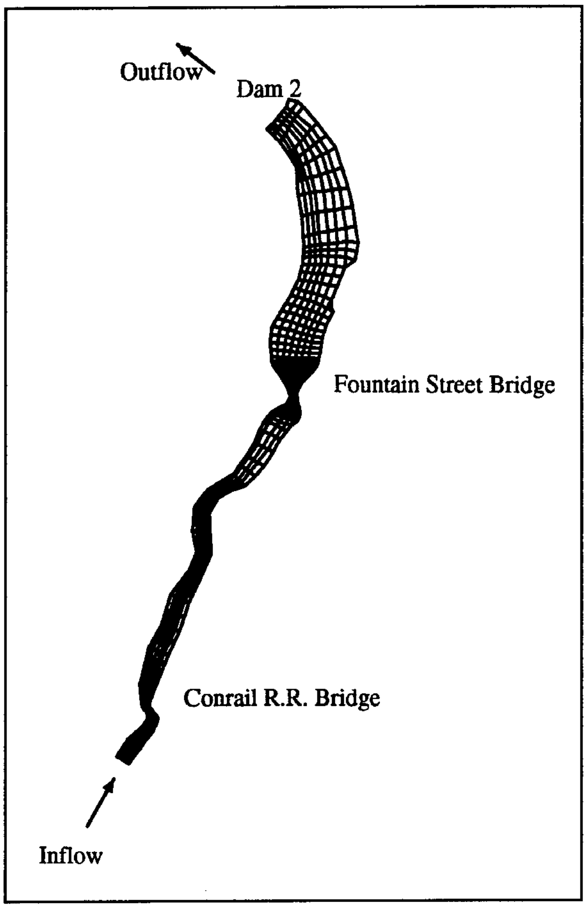

Figure 21. Reservoir 2 finite element mesh, dam break simulation

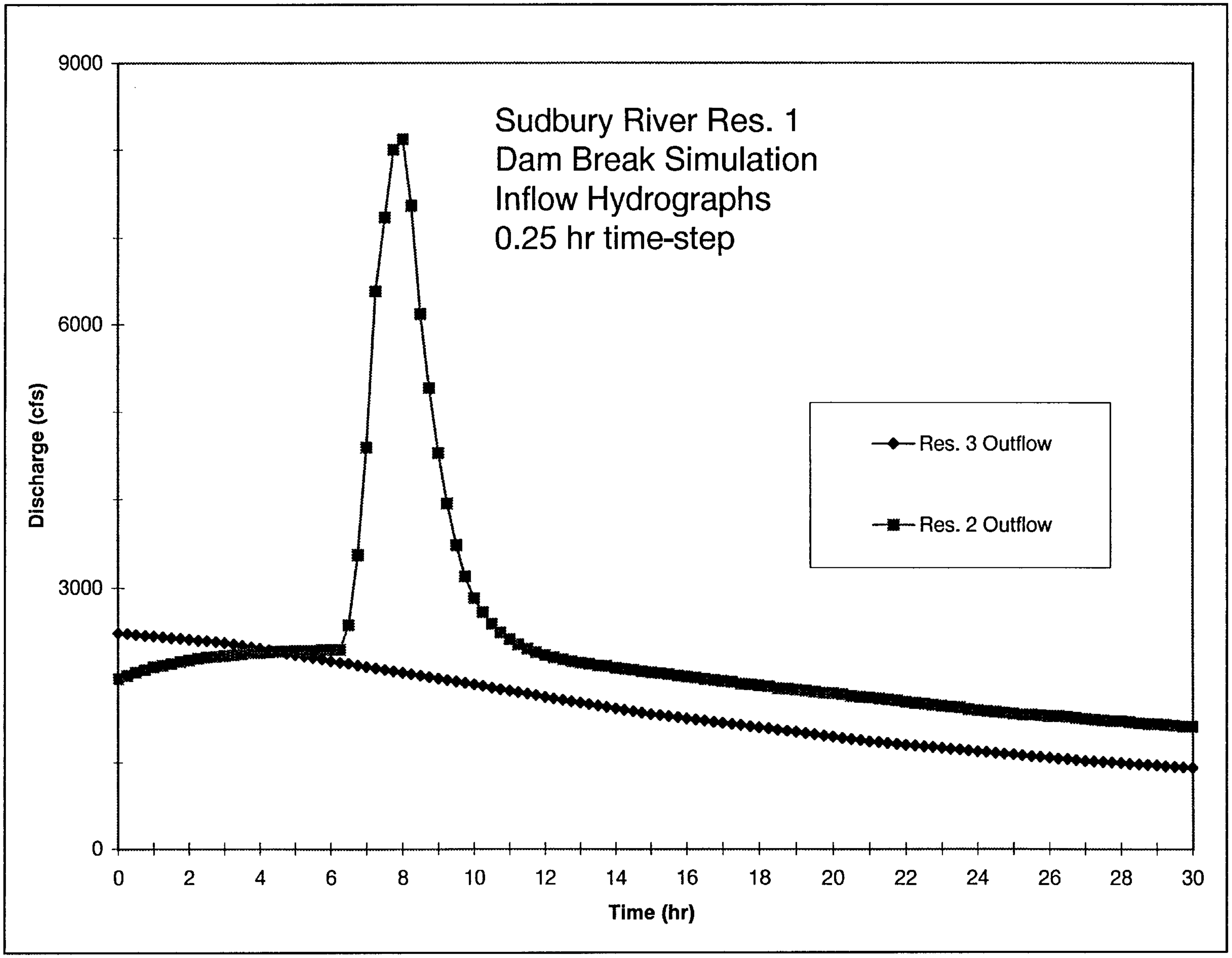

Figure 22. Inflows versus time for Reservoir 1, dam break simulation (Discharge is in cubic feet per second. To convert to cubic meters per second, multiply by 0.0283)

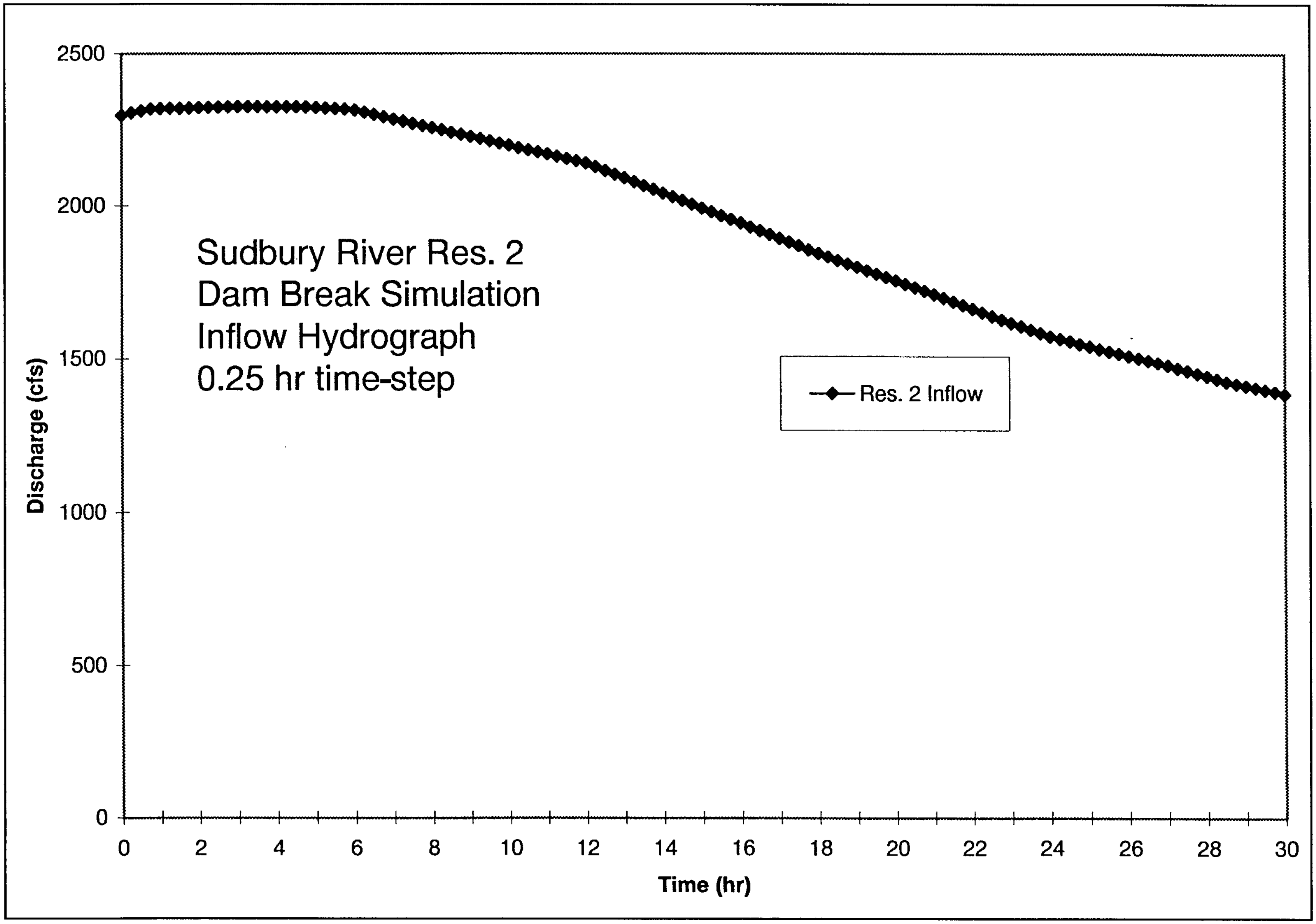

Figure 23. Inflows versus time for Reservoir 2, dam break simulation (Discharge is in cubic feet per second. To convert to cubic meters per second, multiply by 0.0283)

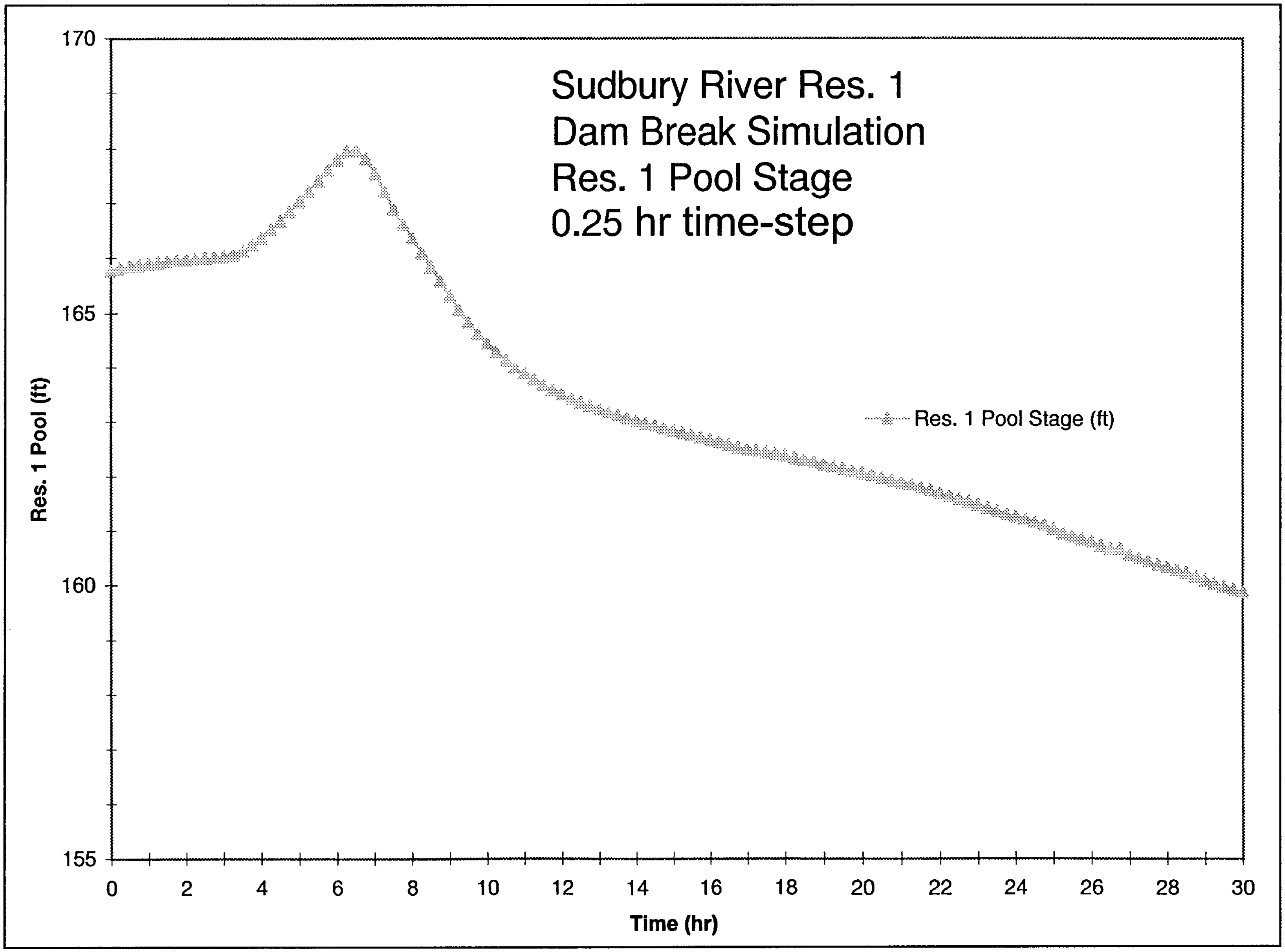

Figure 24. Pool stage versus time for Reservoir 1, dam break simulation (Discharge is in cubic feet per second. To convert to cubic meters per second, multiply by 0.0283)

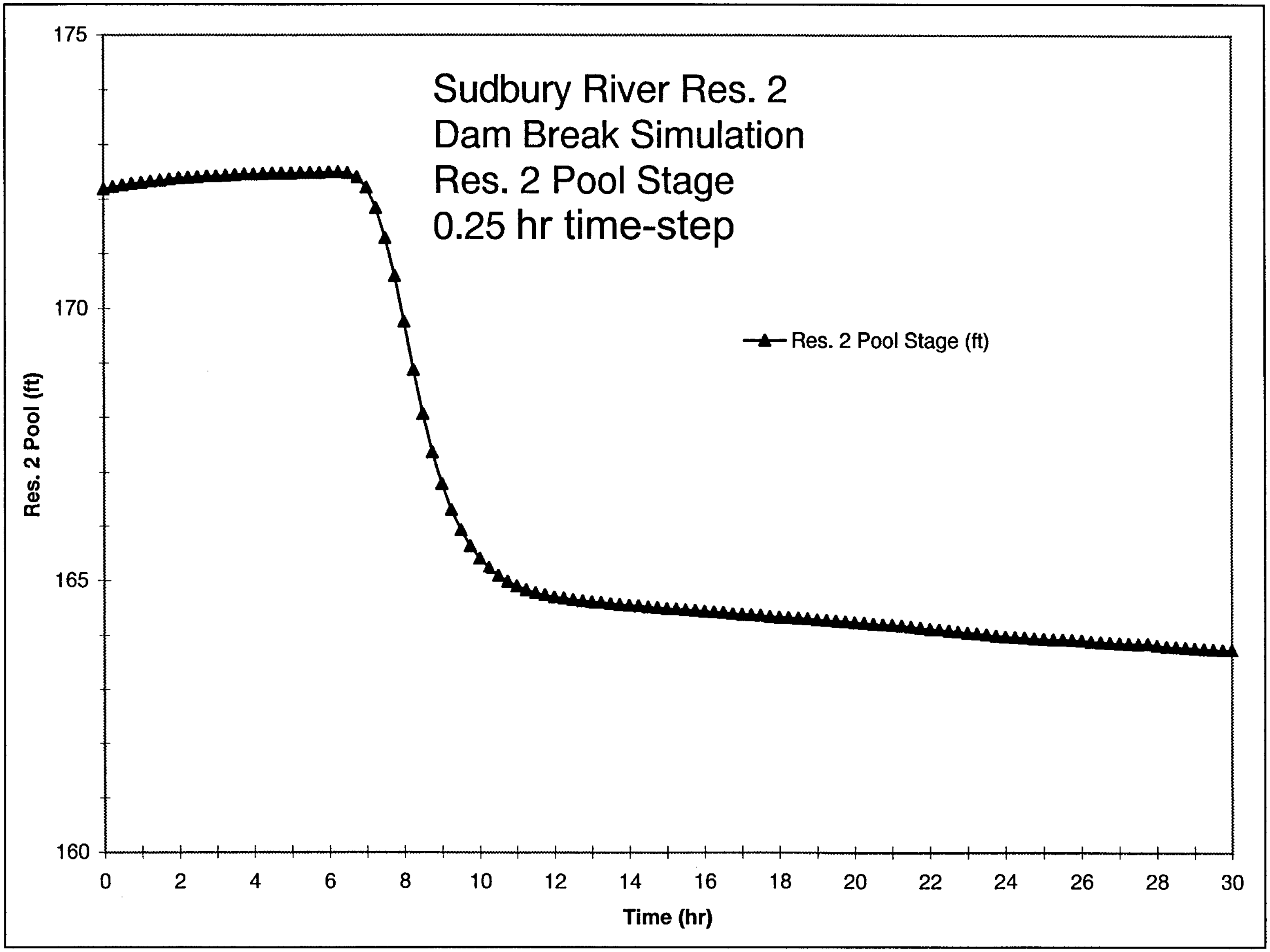

Figure 25. Pool stage versus time for Reservoir 2, dam break simulation (Discharge is in cubic feet per second. To convert to cubic meters per second, multiply by 0.0283)

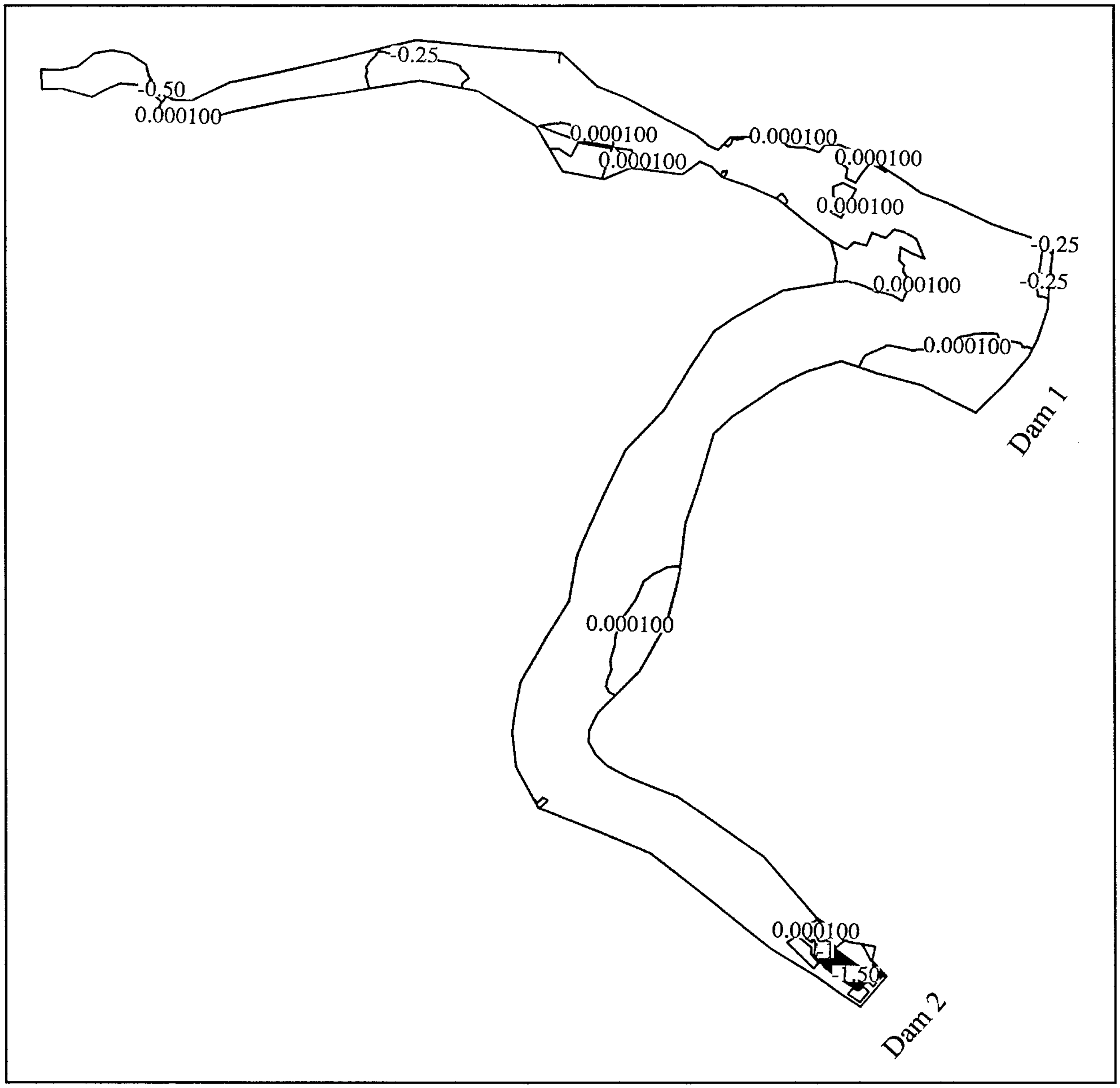

Figure 26. Contours of cumulative bed elevation change (ft), contour interval 0.25 ft, dam break simulation (hour 30) Reservoir 1

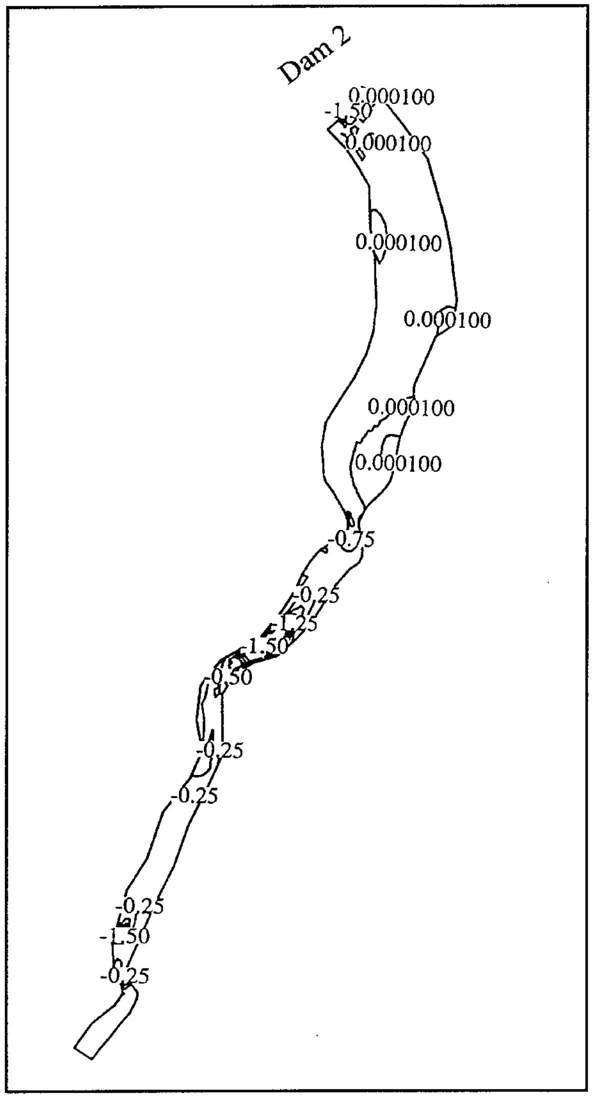

Figure 27. Contours of cumulative bed elevation change (ft), contour interval 0.25 ft, dam break simulation (hour 30) Reservoir 2

REPORT DOCUMENTATION PAGE	Form Approved OMB No. 0704-0188

1. REPORT DATE *(DD-MM-YYYY)* August 2001	**2. REPORT TYPE** Final Report	**3. DATES COVERED** *(From - To)*
4. TITLE AND SUBTITLE Hydrodynamic and Sediment Transport Study of Sudbury River, Massachusetts; Numerical Model Investigation		**5a. CONTRACT NUMBER** **5b. GRANT NUMBER** **5c. PROGRAM ELEMENT NUMBER**
6. AUTHOR(S) Gregory H. Nail, David D. Abraham		**5d. PROJECT NUMBER** **5e. TASK NUMBER** **5f. WORK UNIT NUMBER**
7. PERFORMING ORGANIZATION NAME(S) AND ADDRESS(ES) U.S. Army Engineer Research and Development Center Coastal and Hydraulics Laboratory 3909 Halls Ferry Road Vicksburg, MS 39180-6199		**8. PERFORMING ORGANIZATION REPORT NUMBER** ERDC/CHL TR-01-15
9. SPONSORING / MONITORING AGENCY NAME(S) AND ADDRESS(ES) U.S. Army Engineer District, New England 696 Virginia Road Concord, MA 01742		**10. SPONSOR/MONITOR'S ACRONYM(S)** **11. SPONSOR/MONITOR'S REPORT NUMBER(S)**

12. DISTRIBUTION / AVAILABILITY STATEMENT
Approved for public release; distribution is unlimited.

13. SUPPLEMENTARY NOTES

14. ABSTRACT

Numerical models were used to determine the transport potential for contaminated sediments in two reaches of the Sudbury River near Framingham, Massachusetts. These two reaches are comprised of two small (narrow) reservoirs, one discharging into the other. They are essentially riverine in nature at flows characteristic of this study. A computational hydrodynamic model (RMA2) of the reaches was developed. Several known worst case flood conditions were simulated and the model verified. A sediment transport model (SED2D) was then run using the hydrodynamic responses as the driving force to erode, transport, and deposit sediments. The results of the simulation indicate a potential movement of contaminated sediments in the constricted and shallow areas of the reservoirs for the Standard Project Flood (SPF) conditions. For the lower flow test conditions, 3-year, 14-year, and 100-year flood frequencies, the numerical model computer simulations predicted movement of only negligible amounts of contaminated sediments. Only at the highest flow conditions (SPF) was the movement of sediment considered significant.

15. SUBJECT TERMS

16. SECURITY CLASSIFICATION OF:			17. LIMITATION OF ABSTRACT	18. NUMBER OF PAGES	19a. NAME OF RESPONSIBLE PERSON
a. REPORT	**b. ABSTRACT**	**c. THIS PAGE**			**19b. TELEPHONE NUMBER** *(include area code)*
UNCLASSIFIED		UNCLASSIFIED		49	

Standard Form 298 (Rev. 8-98)
Prescribed by ANSI Std. 239.18